Universidade de Aveiro
2018

Departamento de Eletrónica,
Telecomunicações e Informática

Catarina Isabel
Póvoa Santa Comba

Bengala de apoio a cegos

Cane for the visually impaired

Universidade de Aveiro
Departamento de Eletrónica, Telecomunicações e Informática
2018

Catarina Isabel Póvoa Santa Comba

Bengala de apoio a cegos

Cane for the visually impaired

"*In the middle of every difficulty lies opportunity.*"

— Albert Einstein

Universidade de Aveiro
2018

Departamento de Eletrónica,
Telecomunicações e Informática

Catarina Isabel
Póvoa Santa Comba

Bengala de apoio a cegos

Cane for the visually impaired

Dissertação apresentada à Universidade de Aveiro para cumprimento dos requisitos necessários à obtenção do grau de Mestre em Engenharia Eletrónica e Telecomunicações, realizada sob a orientação científica do Doutor José Manuel Neto Vieira, Professor do Departamento de Eletrónica, Telecomunicações e Informática da Universidade de Aveiro.

Aos meus pais e à minha irmã pelo apoio incondicional.

o júri / the jury

presidente / president

Professora Doutora Ana Maria Perfeito Tomé
Professora Associada da Universidade de Aveiro

vogais / examiners committee

Professor Doutor Salviano Filipe Silva Pinto Soares
Professor Auxiliar do Departamento de Engenharias da ECT da Universidade de Trás-os-Montes e Alto Douro

Professor Doutor José Manuel Neto Vieira
Professor Auxiliar do Departamento de Eletrónica, Telecomunicações e Informática da Universidade de Aveiro (Orientador)

agradecimentos /
acknowledgements

Em primeiro lugar gostaria de agradecer ao meu orientador, Professor Doutor José Manuel Neto Vieira por toda a colaboração, disponibilidade e transmissão de conhecimentos que foram imprescindíveis para a realização deste trabalho.
Agradeço aos pilares da minha vida, os meus pais e a minha irmã, que acreditaram em mim desde o primeiro dia. Sou-lhes eternamente grata por todo o suporte e palavras de alento ao longo destes últimos seis anos.
Às minhas queridas amigas Daniela, Sofia e Rita que me acompanharam muito atentamente ao longo de toda esta jornada.
Aos meus colegas do laboratório Eduardo e Pedro que sempre se disponibilizaram para me ajudar.
Por último mas não menos importante, um agradecimento especial ao Pedro Martins por me mostrar uma faceta mais doce da vida.

Palavras Chave Mobilidade; Deficiência visual; Ultra-sons; Impressão 3D

Resumo

A maior dificuldade que as pessoas cegas e com deficiência visual enfrentam no seu dia-a-dia é serem capazes de se movimentarem de forma independente e segura no exterior. Por forma a serem efetuados os desvios necessários mantendo o trajecto desejado, é necessário que estas consigam detetar correctamente possíveis perigos ou obstáculos. Embora os dispositivos auxiliares de mobilidade tradicionais, como o cão guia e a bengala branca, tenham demonstrado ser ferramentas valiosas e eficazes em diversas situações, ainda existem casos em que estes meios não são eficazes.
Por este motivo, durante as últimas décadas tem havido um grande investimento na pesquisa e desenvolvimento de dispositivos auxiliares de mobilidade eletrónicos. Na Universidade de Aveiro nos anos de 2008 e 2009 foram também desenvolvidas duas bengalas eletrónicas que utilizavam ultra-sons para detetar buracos, desníveis e escadas. No entanto, em ambos os protótipos foi detetada a existência de acoplamento acústico de sinal entre o transdutor emissor e o transdutor receptor, o que reduzia drasticamente a eficácia de ambos os dispositivos.
Nesta dissertação propõe-se uma solução para este problema usando a impressão 3D também conhecida como manufatura aditiva. Esta tecnologia tem vindo a crescer exponencialmente nos últimos anos e ganhando maior destaque em diversos setores nomeadamente na indústria, engenharia e medicina. Neste caso em específico foi usada para produzir vários protótipos de suportes para os transdutores de ultra-sons por forma a minimizar-se ao máximo o acoplamento acústico.

Keywords Mobility; Visually impaired; Ultrasounds; 3D printing

Abstract

The biggest struggle that visually impaired and blind people face on their daily basis is the ability to navigate outdoors independently and safely. In order to make the necessary deviations while maintaining the desired course, it is necessary that visually impaired travellers are capable of correctly detect possible hazards or obstacles. Even though the traditional mobility aids such as the guide dog and the white cane have proven to be valuable and effective tools in many mobility tasks, there are still situations where these means are not effective.

Therefore, in the last decades, there has been a great investment in the research and development of electronic travel aids. At the University of Aveiro in the years of 2008 and 2009, were also developed two electronic canes which used ultrasounds to detect holes, drop-offs, and steps. However, in both prototypes, it was detected the presence of acoustic coupling of the signal between the emitter and receiver transducers which reduced drastically the efficiency of both devices.

Thus, in this master thesis, it is proposed a solution to this issue using 3D printing also known as additive manufacturing. This technology has been growing exponentially in the last years and gaining prominence in several sectors such as industry, engineering, and medicine. In this specific case, it will be utilized to produced several prototypes of supports for the ultrasonic transducers in order to minimize the acoustic coupling.

Contents

List of Figures

List of Tables

List of Acronyms

CAD	Computer Aided Design
CAE	Computer Aided Engineering
CAM	Computer Aided Machining
ETA	Electronic Travel Aids
FDM	Fused Deposition Modeling
HIFU	High Intensity Focused Ultrasound
MATLAB	MATrix LABoratory
STL	Stereolithography
TOF	Time of flight
USB	Universal Serial Bus
VI	Visually impaired

CHAPTER 1

Introduction

According to statistics from the World Health Organization, it is estimated that globally 1.3 billion people are visually impaired (VI), out of which 39 million are blind and 217 million have moderate to severe vision impairment [1].

On the daily basis, blind and visually impaired people face several accessibility and mobility problems while navigating. These problems are related with avoiding obstacles, locating position, finding a pathway and accessing information.

Thus, the need for navigation assistants will always be a constant. Nowadays the white cane and the guide dogs are the most used ones, however, each one of these solutions has its own limitations. To start with, the traditional white cane only provides information on a range of 0.5 meters and it cannot sense any obstacles above the waist level since it requires contact with the obstacles to sense them. On the other hand, there are the guide dogs which are expensive, need an extensive training and ultimately, they have a shorter life than humans[2][3].

Over the past decades, many researchers with the development of the radar and sonar technologies have worked on devices to aid blind people. These devices are called Electronic Travel Aids (ETA). The ETA acquire information about the surrounding environment which would be normally obtained through the visual sense and convert it into information that can be heard or felt by blind people. In other words, these devices are meant to help blind people to overcome problems related to spatial and geographical orientation during their everyday activities. Unfortunately, until these days none of the developed devices have been accepted in the blind community due to the various challenges inherent when using these tools in the real world. Most of these devices, in addition to having an excessive weight and size, had a poor performance and, often the information provided was not reliable or did not suit the needs of the visually impaired at the current situation.

To tackle these issues, in the University of Aveiro were also developed in the years of 2008 and 2009 two ETA, more specifically, two electronic white walking sticks that used ultrasounds to detect obstacles and holes on the ground [4][5]. However in both prototypes it was detected the presence of the acoustic coupling between the ultrasound emitter and receivers. This phenomenon appears whenever a receiver transducer detects a ultrasound signal that is not reflected from its intended target but caused by acoustic coupling. As a consequence, it caused false distance measurements thus reducing the efficiency of both prototypes. The ultrasound waves which originates this effect can be propagated throught the air, by mechanical means and throught the rear of the emitter transducer.

1.1 OBJECTIVES

The aim of this dissertation is to solve the problem of the acoustic coupling of the signal between the ultrasonic transducers. To meet this need, the proposed solution involves the use of 3D printing.

3D printing or *additive manufacturing* are general terms used to designate a wide variety of technologies that allow the creation of objects based on a digital model. These technologies provide countless possibilities and advantages when compared to the traditional methods of manufacturing. This tool enables the creation and full customization of products according to specific needs and requirements that would be difficult to obtain using other production methods.

Although the access to 3D printers for a common citizen is quite restricted, these are already used in some educational institutions namely in the University of Aveiro where the first Portuguese 3D printer was created [6]. In laboratory applications, this tool has many advantages since it allows to produce custom-made pieces in a fast and efficient way.

In this particular case, 3D printing will be used in the creation of transducer supports to prevent ultrasounds from propagating directly from the emitter transducer to the receiver transducer. Having this in mind, it will also be studied the ideal configuration of these supports and which materials can be used in order to eliminate this negative effect.

1.2 STRUCTURE

This document was divided into five chapters and a brief description of each one is given below.

- **Chapter 1** - The current chapter presents a framework of the theme of the master thesis as well as the objectives established and the technology used.
- **Chapter 2** This chapter begins by introducing a brief description of the discovery and development of ultrasounds in the last decades until now. Afterwards, some applications of ultrasounds in industry, medicine and nature are presented. Considering the concept of echolocation it is explained how distances can be measured using ultrasounds. Lastly, it is presented a more detailed description of the acoustic coupling and its origins.
- **Chapter 3** - In this chapter are presented some of the various *electronic aid devices* developed during the last decades and, some commercial versions which are still available for sell in the market.
- **Chapter 4** In this chapter, an analogy is made between the simulation process and the development of prototypes using 3D printing. This chapter is devoted entirely to the experimental process, including the choice of transducer supports to be printed, the software and hardware used, the tests performed, and the decisions made during the experiments. The final prototype is also presented.
- **Chapter 5** - This chapter focuses on the conclusions drawn from the work done as well as some considerations about future work.

CHAPTER 2

The ultrasounds

According to Oxford's Physics dictionary, the sound is *"a vibration in an elastic medium at a frequency and intensity that is capable of being heard by the human ear. The frequency of sound lies in the range 20-20000 Hz[...]"*[7]. Sound waves with a frequency below 20 Hz are classified as infrasounds and those with a frequency beyond the upper limit are referred to as ultrasounds or ultrasonics.

Even though ultrasounds are not used in oral communication between human beings, these are utilized in a wide range of applications such as medicine and industry. Ultrasonic applications can be divided into two distinct categories: low and high power ultrasonics. Concerning low power ultrasonics, these are used as a way of studying materials or as a method of control[8]. This is accomplished without any structural changes in the propagating material. A widely known example is medical imaging. On the other hand, the function of high power ultrasonics is to modify the material in which the ultrasonic wave is propagating. High power ultrasonics are used per example in medical therapy, surgery and, ultrasonic cleaning.

The focus of this chapter are the ultrasound waves starting with a brief introduction of the historical development of these sound waves and the respective applications throughout the past centuries.

Afterwards, in section 2.2 are introduced some of the current applications of the ultrasounds in the industry and in medicine and their advantages. At the end of this section are also presented some animals that use their ability to emit ultrasounds to move around and communicate.

The function of the ultrasound transducers and the method of measuring distances using ultrasounds are explained in section 2.3.

This chapter finishes in section 2.4 with a more detailed description of the problem which originated this master thesis, that is, the acoustic coupling between the emitter and receiver transducers.

2.1 HISTORICAL DEVELOPMENT

It it not known the moment at which the human being became aware of the existence of sounds above their limits of hearing since there are no records of investigation before the 19th century. Although the study of ultrasound has only begun in that century it can be said that the next 100 years were crucial to create foundations for the growth and development of ultrasounds in the 20th century.

The two major discoveries that had a dominant impact on the 20th century ultrasonics, were made during the 19th century. The first was made by Joule in 1847 who discovered magnetostriction, which means, changing the dimensions of a ferromagnetic material such as iron or nickel when subjected to a magnetic field. The second occurred in 1880 when the Curie brothers discovered piezoelectric properties in some crystals. Piezoelectricity refers to electrical charges that are developed in some types of crystals when subjected to pressures or tensions [9][10]. Thanks to the discovery of piezoelectricity and magnetostrictive effects it was then possible to generate and detect ultrasounds.

In 1912 after the sinking of the Titanic there were several scientists who sought to discover acoustic ways to detect submerged obstacles. However, the study of ultrasounds as a specific branch of science only began during World War 1 due to the need of Allied forces to detect German submarines[10].

It was only by the end of the First World War that a former student of Pierre Curie named Paul Langevin invented the quartz ultrasonic transducer. He thus became the father of the underwater SONAR and his ideas were extensively utilized by the Americans and the French[11][12][13].

The sonar, also called Anti-Submarine Detection Investigation Commitee (ASDIC), consisted on a transmitter that would sent a sound wave through the water. If the wave hit any target it would be reflected and detected by a receiver. The time between sending the sound wave until receiving the reflection allowed to calculate the range to the target [14][15].

Between the two wars, the main focus was directed towards the development of ultrasounds of high intensity including whistles, electric spark-devices, and sirens [16]. It is necessary to highlight the work developed by Wood and Loomis during this period in the study of the effects of intense ultrasounds[9]. Between 1927 and 1939 there was an immense application of high-intensity ultrasounds in the most diverse fields.

During the years 1940-1955, there was a great development of the technology. They include [17][18]:

- Development of the modern horn transducer by Mason in 1950;
- Appearance of the concept of a prestressed sandwich transducer;
- Appearance of major processes like ultrasonic cutting, cleaning, soldering and metal welding;
- Discovery of ultrasonic drilling and cleaning;
- Ultrasonics for medical purposes such as ultrasonic therapy. Ultrasounds were also used for diagnostic purposes.

Since 1970, ultrasonic technologies suffered rapid and extensive advances due to a significant improvement of theoretical analysis [9]. In the field of high frequency, it stands out the invention of the ultrasonic scanning microscope by Lemons and Quate in 1974 [10]. Between 1970 and 1980 in medical ultrasounds, it was possible to scan a fetus in a pregnant woman as well as measuring the blood flow [19].

2.2 APPLICATIONS OF ULTRASOUNDS

2.2.1 IN INDUSTRY

In the industry, the oldest and most important commercial application of ultrasounds is the ultrasonic cleaning. This process is composed by a tank filled with a proper cleaning fluid under which are connected piezoelectric transducers calibrated to oscillate at a given frequency. By applying an alternated current to the piezoelectric crystals, vibrations are generated in the tank and consequently, all the material in its interior is cleaned up. The main advantage of this process over the tradicional ones like brushes is that it can reach places otherwise inaccessible [20].

Figure 2.1: Ultrasonic cleaner. Source:[21]

Another major industrial application is the welding of thermoplastics which is considered to be fast, clean and easily automated. This process requires very high intensities, generally up to 90kHz and, it is primarily a thermal operation allied with a steady pressure and a large oscillatory amplitude. In plastic welding, the plastic at the target join is melted and consequently, the two parts are joined. It is often used in the production of plastic toys, sealing of plastic bottle caps and manufacture of electrical goods.

In the last years, ultrasonic cutting has been utilized in a variety of industries since it allows a highly precise cut in several kinds of material such as bones, multi-layered fabrics and even confectionery. This technique reduces the amount of waste produced as wells as the process time comparatively to conventional methods. Since the middle of the 1990s, ultrasonic cutting has been used in the food industry because some goods can be extremely difficult to cut by non-ultrasonic cutting methods due to their texture and structure [22].

Besides ultrasonic cutting of food, the use of this technology in the food industry also includes food preservation. In this case, ultrasonic waves are utilized to break down bacterial cell walls. The application of ultrasonics in this process significantly reduces the amount of chemicals or heat added to the food.

Lastly, ultrasonic waves can be used to test components non-destructively, more specifically, to detect internal flaws or discontinuities within ferrous or non-ferrous materials.

2.2.2 IN MEDICINE

Medical applications of ultrasounds can be divided into 2 distinct groups: diagnosis, also called sonography, and therapy [9].

In medicine, in the diagnosis category, it can be found one of the most important applications of the ultrasounds which is the ultrasound. Through this technology, it is possible to obtain images of internal organs and tissues and thus evaluate their condition. Nowadays, it is used as a complement to x-ray exam due to its ability to detect details that go unnoticed by the x-rays. Since ultrasound does not use ionizing radiation it does not bring any risks to the health of patients.

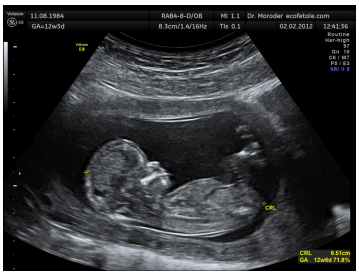

Figure 2.2: Ultrasound image of a fetus at 12 weeks of pregnancy. Source:[23]

On the other hand, the therapy uses high-intensity waves to cause physical changes in the patient in order to improve their health [9]. An innovative therapeutic technique is the *HIFU* also known as *High Intensity Focused Ultrasound*. This procedure was originally used to treat prostate cancer and uses high-frequency ultrasounds to destroy cancer cells through thermal absorption[24]. The duration of each session can vary between 1-30 seconds[25]. Ultrasounds also have been used in rheumatology since the heat caused by these waves favors the regeneration of the tissues, as well as, the muscular strengthening of the damaged area.

2.2.3 IN NATURE

In nature, there are several animals capable of hearing and producing ultrasounds. It was back in 1794 that Lazzaro Spallanzani first found out the ability of bats to navigate across obstacles in the dark or even blindly. However, it was only in 1938 that Pierce and Griffin detected the ultrasonic signals produced by bats. In the next 20 years along with other collaborators, they continued to study this phenomenon and since then a lot of information has been discovered regarding echolocation [26].

Echolocation, also called bio sonar, is a physiological process used by some animals to detect and localize obstacles. Echolocation in animals consists of the production and emission of a series of ultrasonic pulses and through the received echoes, of their strength and delays perceive the distance to the obstacles[27].

One of the animals best known for its echolocation capability is the bat. Bats produce echolocation calls through their mouths and sometimes through their noses and through the reflected echoes they can create an acoustic map of the objects around them [28]. Their ears have also a very important function because they can move dynamically in order to improve the detection of echoes in specific directions [29].

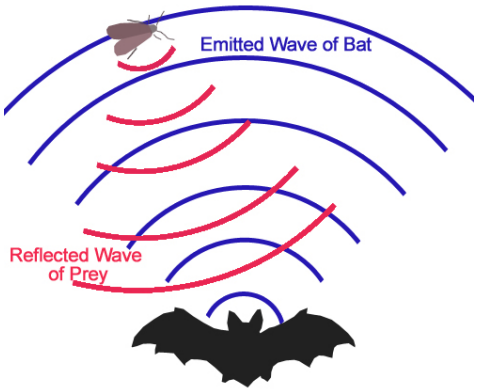

Figure 2.3: Representation of echolocation of bats. Source:[28]

Sea animals are also known for their echolocation capabilities. Many toothed whales species, such as dolphins, produce short clicks(50-100 μs) for hunting and acquire information about the surrounding environment. Marine animals are at advantage over terrestrial animals since the attenuation in water is smaller than in the air, which leads to an increase in the range of location [10].

2.3 MEASUREMENT OF DISTANCES USING ULTRASOUNDS

The heart of any ultrasound system is the transducer which is a device capable of transforming a type of energy into another, in this case, electric energy into mechanical energy and vice versa. The most commonly used type of transducer is the piezoelectric transducer. This transducer contains a crystal that vibrates when a voltage is applied thus generating a particular frequency response.

A simple and effective way of measuring distances is through ultrasonic sensors. These sensors use the concept of echolocation to calculate relative positions of obstacles. Echolocation consists of the determination of *time of flight* (tof), ie the time elapsed between the emission of the sound waves and the arrival of the echo.

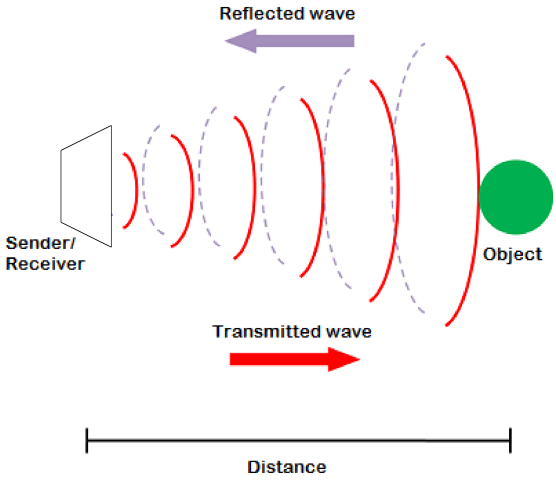

Figure 2.4: Operating principle of a ultrasonic sensor. Adapted from:[30]

Thus, when transmitting an ultrasound pulse it is possible to calculate the distance to an object by measuring the time t in seconds taken for a reflected echo to be received. Considering that the measured time corresponds to the outward and return paths, the distance d in meters is given by (2.1):

$$d = \frac{t * c}{2} \tag{2.1}$$

where, c is the velocity of sound as it propagates through an elastic medium.

Sound speed is also closely related to the density of the medium in which it propagates, per example, the speed of sound is lower at denser materials. Another factor that affects the velocity of sound is temperature. The relationship between sound speed and temperature T is given by the formula (2.2):

$$c = 331.4 + 0.6T \tag{2.2}$$

Thus, at room temperature, the velocity of the sound is about 344 m/s.

Although the process of measuring distances with ultrasounds is quite simple, there are other factors which need special attention since they can affect the measurements.

To begin with, the transducer has a minimum sensing range also known as the blind zone. This corresponds to an area in front of this device where it is not possible to obtain a reliable measurement because even after the signal transmission is complete, the transducer continues to vibrate. Therefore, it is not possible to receive any echo immediately after to avoid coupling between both signals. In figure 2.5 it is possible to visualize the blind zone, as well as, the sensing range where the detection of objects is possible.

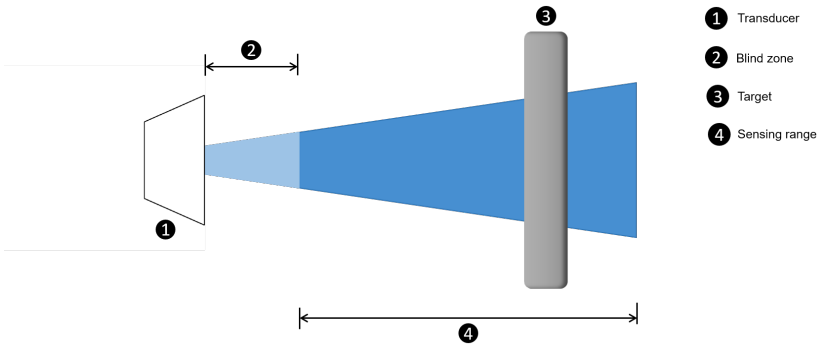

Figure 2.5: Transducer's operation. Adapted from:[31]

Lastly, attenuation and reflection phenomenons can also affect the correct obtainment of a distance d due to the following factors:

- Dimensions of the object

  The higher the target the higher the reflected wave energy and consequently the greater the detection distance possible;

- Materials

  Wood, metal, concrete, glass and paper objects can reflect approximately 100% of the ultrasonic waves. On the other hand, clothing, cotton and wool are very difficult to detect since they absorb some of the ultrasounds. These can only be detected short distance;

- Surface of target

  Objects with irregular or porous surfaces such as felt or sponge cause the dispersion of the beam and therefore may not be detected.

2.4 ACOUSTIC COUPLING OF THE SIGNAL

The acoustic coupling of the signal occurs when two ultrasonic transducers, one emitter and one receiver, are in close proximity and part of the signal being transmitted leaks to the receiver transducer. Since it is not possible for the receiver to know that the signal acquired is not a reflected echo, the time of flight measured is incorrect and consequently, it is not possible to detect obstacles accurately. Therefore, this phenomenon has negative effects on the performance and response of the transducers.

In figure 2.6 is represented the principle of distance measurement using two ultrasonic transducers, where the transducer T represents the transmitter and R is the receiver.

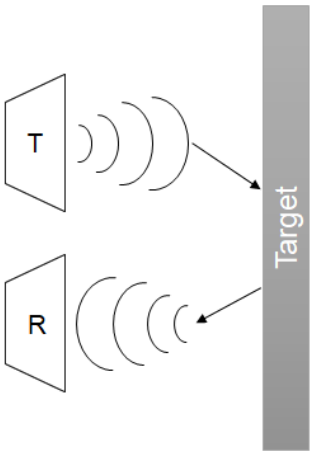

Figure 2.6: Measurement of distances using ultrasounds.

The presence of the acoustic coupling of the signal can be observed in figure 2.7, where the first pulse corresponds to this negative effect and the second one to a reflected echo.

These signals were acquired using one of the several 3D supports designed throughout this work when the transmitter transducer was sending a short pulse. As it can be seen the pulse corresponding to the acoustic coupling remains approximately constant throughout the time.

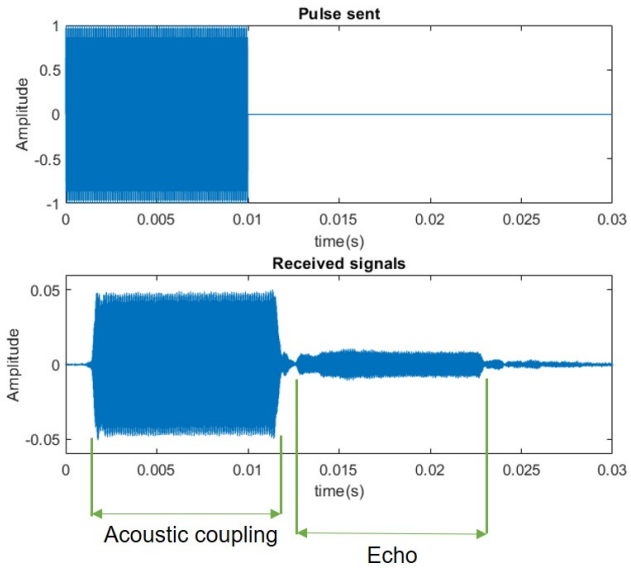

Figure 2.7: Pulse sent and received echo affected with acoustic coupling.

The problem inherent to the acoustic coupling becomes more perceptible when applying a matched filter. These filters are typically used in radar for distance measurement and are obtained by correlating a known signal with an unknown signal. The aim of the matched filters is to detect the presence of the known signal in the unknown signal.

In this specific case a matched filter was obtained by correlating the pulse sent from figure 2.7 with the respective signals received. If the output of the filter exceeds a certain threshold it can be concluded that the received signal is in fact a reflected echo. In figure 2.8, it is notorious that the magnitude of the acoustic coupling is superior comparatively to the magnitude of the reflected echo. Thus, it is not possible to correctly detect the presence of obstacles. On the other hand, if the echo arrives too early, both the acoustic coupling and the echo signals overlap making it also impossible to accurately detect obstacles.

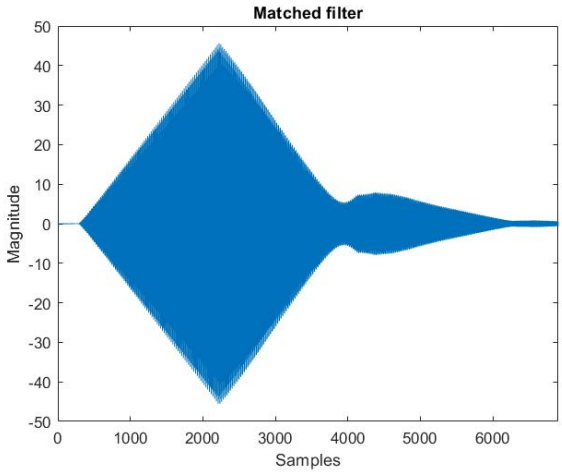

Figure 2.8: Output of the matched filter.

In figure 2.9 is portrayed the acoustic coupling between the two ultrasonic transducers. As stated in the *Introduction*, the ultrasound signal that originates this phenomenon can reach the receiver by three different means which are represented by $H_1(s)$, $H_2(s)$ and $H_3(s)$.

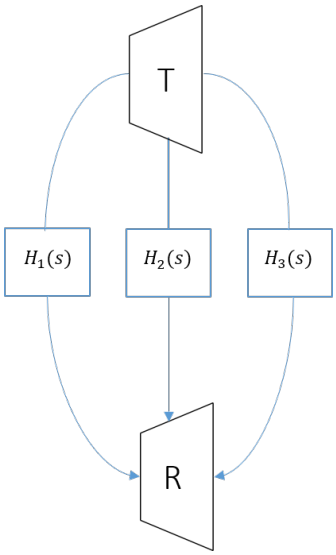

Figure 2.9: Model of the three sources of the acoustic coupling.

The $H_1(s)$ illustrates the acoustic coupling through the rear of the transducers, the $H_2(s)$ refers to the acoustic coupling with mechanical origin and $H_3(s)$ corresponds to the acoustic coupling through the air.

The figure 2.10 presents one of the many versions of the 3D supports created and in which it is represented the three different ways in which the ultrasound signal propagates. Once again, the upper transducer corresponds to the transmitter and the lower one to the receiver.

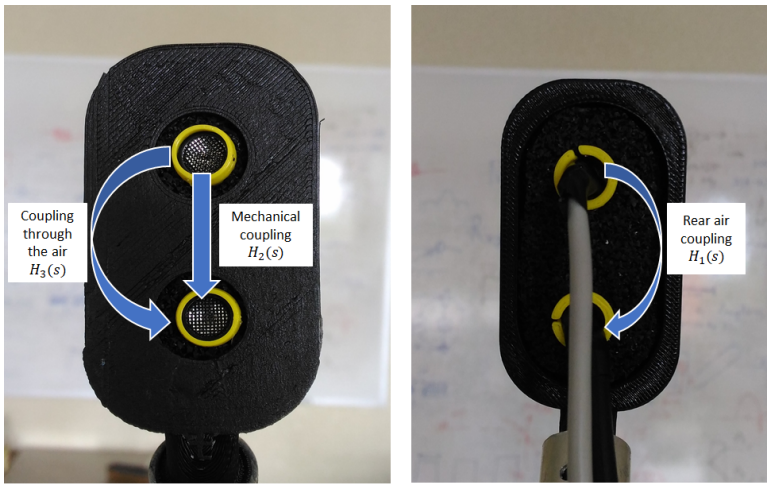

(a) Front part of 3D piece

(b) Rear part of the 3D piece

Figure 2.10: Real model of the acoustic coupling.

The acoustic coupling through mechanical means $H_2(s)$ results from the mechanical interference of the transmitter transducer relatively to the receiver transducer. The emitter transducer during pulse transmission vibrates and consequently, this vibration propagates through the structure between the two transducers being eventually transferred to the receiver transducer.

On the other hand, the acoustic coupling through the air $H_3(s)$ results from the radiation patterns of the emitter and receiver transducers. Since their radiation diagrams aren't zero for 90° it occurs interference between both transducers which causes the frontal acoustic coupling.

Finally, on the back of the emitter, there may be signal losses during signal transmission which can be detected by the receiver causing the acoustic coupling through the rear of the transducers $H_1(s)$.

CHAPTER 3

Electronic Travel Aids

When in movement, blind and visual impaired people face several challenges to get from one place to another safely, efficiently and with dignity. One of their biggest difficulties is avoiding obstacles along the way. These obstacles include stationary objects like posts, walls, and vehicles and also moving objects such as pedestrians or even hazards such as steps or icy patches. Another challenge is related to spatial localization and the establishment of a route to follow in order to go from the current location to the desired destination.

In that sense, given the limitations associated with traditional navigation assistants, several electronic aid devices have been developed throughout the last four decades. These devices can be classified as primary or secondary aids. The primary aids are devices which can be used alone since they provide enough information for the user to move around safely and independently. The most widely known primary aids are the guide dogs and the white cane. In addition to these two familiar examples, there are also the LaserCane and the K-sonar which will be later presented in this section. Regarding the secondary aids, these cannot be used by themselves because the information which they provide isn't sufficient for the user to move around without the risk of being hurt.

These devices besides providing spatial information about the environment in which the visually impaired person is, must also satisfy some requirements. One of the biggest concerns of the blind people is related to the appearance and characteristics of the *ETA*. These devices should be discrete, light-weighted and preferably consist of a single unit. Besides these aspects, it is also required that these are robust enough to be used both on outdoors and indoors, as well as, being capable to withstand different weather conditions. Concerning the operation mode of these aids, it is essential that they are easy to use and do not require an extensive period of training. It is also fundamental that their maintenance is simply to execute. Of all the requirements listed above, the one that is considered by the blind community to be the most important is the consistency of the information. This means that the information provided to the user at the equivalent time and at the same location must be the same otherwise the blind people will quickly dismiss the aid device [32].

This chapter presents some of the most important developed *ETA* with a brief description of each one of them. These systems are organized based on the type of the information which they provide to the blind user. The first two provide audio feedback and the following eight use tactile information. Finally, at section 3.2, a representative selection of electronic aid devices which are still available in the market are presented.

3.1 DEVELOPED ETAS

3.1.1 NAVBELT

NavBelt was developed in the University of Michigan and, it is a guidance system which includes a belt with an array of ultrasonic sensors mounted on it, a small portable computer and stereophonic headphones. This device uses navigation and obstacle avoidance technologies which were originally designed for robots.

The computer receives the information from the eight ultrasonic sensors and creates an angle map and the corresponding distance of any obstacle at each angle. Afterwards, the information is transmitted to the user through the stereo headphones and the obstacle avoidance algorithm produces the sounds corresponding to each mode. The NavBelt has two different operational modes based on the type of information offered to the blind user: the guidance and the image mode. In the guidance mode, the computer knows the blind user final destination and guides him in terms of the direction to follow. On the other mode, it is created a panoramic virtual image of the environment in which, eight tones with different amplitudes ae played successively from eight different virtual direction. Then, these maps are translated to sounds which are heard and interpreted by the user [33].

This system besides having an voluminous size, it also requires extensive periods of training so that the blind person is be capable of understanding the guidance signals.

Figure 3.1: Transducer's operation. Source:[33]

3.1.2 THE VOICE

The vOICe system is a software which claims being able to substitue sound for low-vision. This software can be run on any computer with a camera and, it works by converting the pictures captured from the camera into a sound mapping. The alert messages consist on a series of beeps and whistles which are sent directly to the user through a pair of headphones [32].

Figure 3.2: Typical set-up of the vOICe system. Source:[34]

The system is light-weighted, discrete and easy to wear but it blocks both visually impaired ears. Other than that, it requires an extensive period of training so that the user is able to interpret the different sound patterns [34].

3.1.3 GUIDECANE

GuideCane was developed in the University of Michigan's Mobile Robotics Lab and is an update of NavBelt [33].

This device has the same components and algorithms of the Navbelt with the difference that the ultrasonic sensors are mounted on the main device which has wheels. There is also a cane which is attatched with the main device allowing the blind user to push it through along the way. The principle of operation is quite simple: when an obstacle is detected the obstacle avoidance algorithm changes the direction of the cane.

The GuideCane analyzes automatically each situation which translates into a period of training almost nonexistent. Even so, it is only capable of scanning a small area and the prototype is still hight weighted and hard to carry around [34]. The prototype sketch is visible in figure3.3.

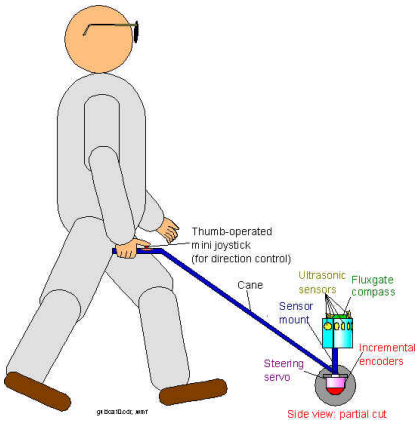

Figure 3.3: GuideCane prototype. Source:[35]

3.1.4 BLIND-GUIDE CANE BASED ON MULTI-SENSORS

It was developed by Yiting Yng and Lunfu Dog in 2015 a guidance system for blind people, able of detecting obstacles not only at the front of the user but also overhead [2].

This device consists on a cane with three ultrasonic sensors and a microcontroller. In figure 3.4 is possible to see the positioning of these sensors, where two of them are meant to detect obstacles in front and the remaining sensor is able to detect obstacles overhead. The microcontroller manages all the transmitted and received signals and based on the decision-making algorithm in case of existing an obstacles it alerts the blind user through vibration or an audio message.

The tests performed demonstrated that this device is capable of accuratly detect objects however its maximum range is only of two meters [36].

Figure 3.4: Positioning of the ultrasonic sensors. Source:[2]

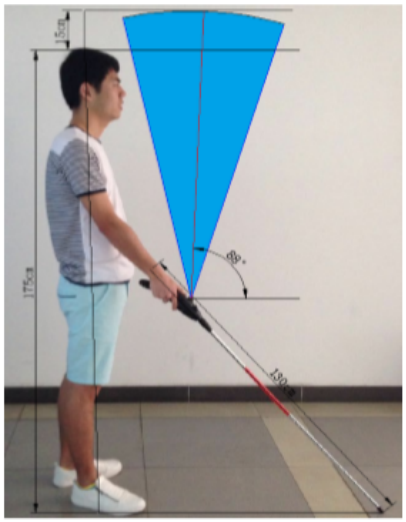

Figure 3.5: Proposed prototype and its detection range. Source:[2]

3.1.5 ELECTRIC LONG CANE (ELC)

In this protoype named as electric long cane(ELC), it was developed an improved version of the traditional white cane [37]. The ELC contains an electronic sensor in the handle of the cane which enables the detection of obstacles above the waistline of the blind person. All the eletronics such as the micromotor, the battery and the microcontroller are also embedded in the handle of the ELC.

When an object is detected by the sensors, a mechanical vibration caused by the micromotor alerts the user about a possible collision. The frequency of vibration increases as the object gets closer.

This device was tested on eight visually impaired people and proved to be effective at detecting several types of physicals barriers wich were located above the waistline. However, since its a navigation device, it is still necessary the usage of another aid which can provide orientation to the blind user [36].

Figure 3.6: Handle of the Electric Long Cane. Source:[37]

3.1.6 FIU PROJECT

This project was developed at Florida International University *(FIU)* and uses a pocket computer to generate 3D spatialized sounds and, according to the readings obtained from a multidirectional sonar system it is capable of detecting obstacles around the blind user.

It formed of two modules: a sonar composed by six ultrasonic range sensors which detects obstacles in six radial directions and, a pocket computer containg a software capable of processing the information coming from the sonar and headphones [38].

In order to associate the signals with the directions being explored by the sonar modules, Head Related Transfer Functions *(HRTF)* are used. This way, the user is capable of creating a mental image of his surroundings and thus avoiding possible obstacles [34].

Figure 3.7: FIU project prototype. Source:[38]

This project was tested inside the Engineering Center at FIU by four blind-folded individuals. Although the obtained results were promising, the navigation speed was rather low. The system though being wearable is not ergonomic and pratical.

3.1.7 CYARM

CyARM is an electronic aid device developed by researchers in Japan that measures and calculates the distance to an obstacle using an ultrasonic sensor [39].

The blind user is alerted of the presence of the obstacle through a tension apllied to a wire that is attached to him (e.g. his belt). The closer the object, the greater the tension that will be. The system is composed of a microcontroller that processes the information and a motor which controls the tension applied.

Figure 3.8: CyARM system. Source: [39]

As strong points, the system has a high detection rate in terms of static obstacles and it is easy to use [34]. On the other hand, for dynamic object the detection rate rapidly decreases and also implies a constant movement to sense the environment.

3.1.8 EPFL PROJECT

This system consists on a wearable device capable of detecting obstacles at the shoulder height using a stereoscopic sonar. The protype is composed by sonar sensors, a microcontroller, eight vibrators and a calibration console (PDA). The information is gathered by the sonar sensors placed on the shoulders of the user and sent to the microcontroller which calculates the distances to the obstacles. The user then receives a vibro-tactile feedback of the position of the nearest obstacles [40].

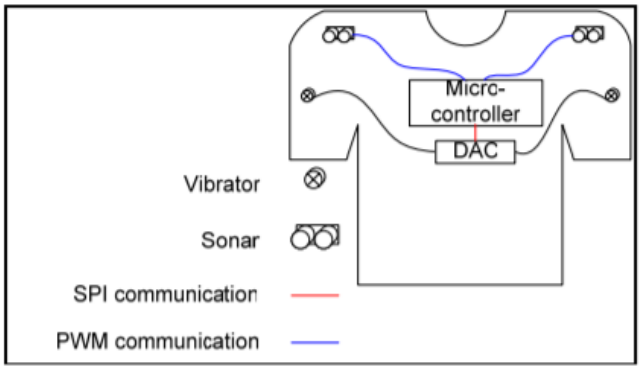

Figure 3.9: System arquitecture. Source:[40]

The system main advantages are associated to its low height, power-consumption and cost. Since it is a hands-free device it allows the user to use a traditional cane, a guide dog or any other device [34].

However, this system was not tested on visually impaired people and in some cases it detected the users hands as an obstacle.

3.1.9 BLAVIGATOR

At the University of Trás-os-Montes e Alto Douro a navigation system for blind people named as Blavigator has been developed [41]. The purpose of this system is to guide the blind user until the desired destination by providing contextual information about his surroundings.

Blavigator consists of a cane that contains an antenna, a RFID reader and a small box containing all the electronic components.

In order to provide spatial information about indoor and outdoor environments, this system uses different technologies such as GPS, RFID, and Wi-Fi [42].

3.1.10 HOLE-DETECTING CANE FOR THE VISUALLY IMPAIRED (V2008 AND V2009)

As described in the Introduction, in 2008 at University of Aveiro it was developed the first prototype of a cane capable of detecting holes, drop-offs and steps [4]. For that purpose, this cane used ultrasound transducers and in case of danger it alerted the user through vibrations. In this version, photovoltaic solar cells were added to the cane to reduce the power-comsumption of the prototype and also to prevent the user from being worried about charging the batteries on a daily basis. In figure 3.10 is

possible to see the prototype from this version, noticing that all eletronic elements were placed inside an external box.

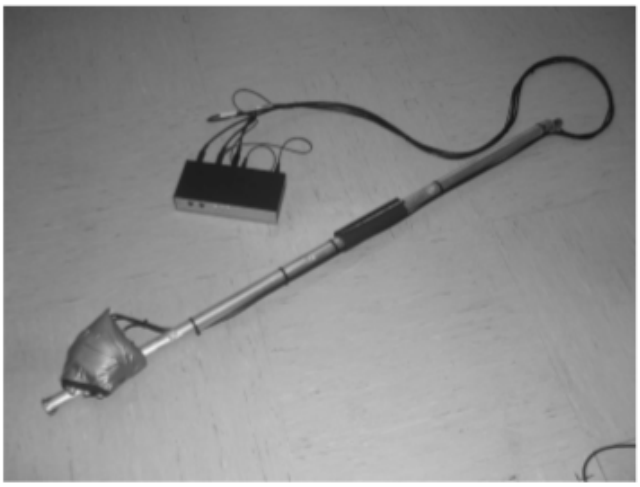

Figure 3.10: Prototype of v2008. Source:[5]

The main drawbacks from this device are related to its excessive weight and to the slow detection algorithm.

In 2009 a whole new prototype was developed which was way lighter and practical compared to the 2008's version. The solar panel was removed, a smaller box containing the electronic components was mounted in the cane and, the obstacle detection algorithm improved.

Futhermore, it were performed test fields to test the viability of the new prototype. The device proved to be an useful tool in walking down stairs and was able of detecting all drop-offs and holes on time. However, in irregular surfaces such as portuguese sidewalk, carpet and grass were detected several false positives. In the figure 3.11 it is possible to see the v2009 being tested by blind people.

Figure 3.11: Test field of the v2009. Source:[5]

3.2 COMMERCIAL PRODUCTS

3.2.1 THE ULTRACANE

The UltraCane is a primary mobility aid, which combines a cane with two ultrasonic sensors built into the handle of this device. One of the sensors is meant to sense the obstacles straight ahead on a range of 2 to 4 meters and, the other one to detect obstacles ahead and upwards up to 1.5 meters. Thanks to the two vibrating buttons present on the handle, it provides tactile feedback to the VI user by varying the intensity of the vibration according to the distance from the obstacle [36][43].

One of its positive aspects is the adaptation period which tends to be short if the blind person is already used to the traditional white cane. Futhermore, besides providing additional information comparatively to the white cane it also leaves the user with a free hand which is an important aspect for the majority of the visually impaired people. This device is available for sale in 10 standard lenghts from 105 cm to 150 cm in the UK and EU with a cost of 635£ [43].

Figure 3.12: The handler of the Ultra Cane. Source: [43]

3.2.2 MINIGUIDE

The Miniguide is a small device designed to be used as a complement to a traditional cane or the guide dog. This contains two transducers, one transmitter to emit short ultrasonic pulses and a receiver to acquire the reflected echoes.

In the begining, there were two distinct versions of this device based on the type of output provided to the user. One version provided an audio output and the other one provided an vibratory output. Since then, these two outputs have been combined resulting on a single device in which the output can be selected alternately. In the audio mode, the Miniguide beeps in order to alert the user of the presence of an obstacle and, the pitch of the beep depends on the distance from the obstacle. On the other hand, in the vibration mode a farther object will traduce on a slow rate of vibration and a close object results in a rapid vibration. Besides that, it has multiple operation modes of detection ranges which makes it appropriate for different environments.

The main strenghts of the Miniguide are related to its flexibility and versability. However, this device can not detect the existence of holes or steps and, since its a complement to the tradicional navigation assistants it leaves the user wihout an empty hand[32].

Figure 3.13: The second version of the Miniguide. Source: [44]

3.2.3 K-SONAR

The K-Sonar is an ultrasonic sensing device that can be attached to the traditional white cane to increase the independence of blind people. Besides the ultrasonic sensor, it is also constituted by a microprocessor that converts the distances into sound signals that are heard by the user through the earphones. These audio warning signals vary according to the distance from the obstacles, that is, high-pitch sounds are associated with distant obstacles and low-pitch sounds to near obstacles [34]. Through these sound associations users are able to identify different obstacles and gather spatial information about the surroundings. One positive aspect of this device is that it can be easily detached from the white cane and used independently. However, similarly to happens with others sonar devices, occasionally the distances measured are incorrect due to the interference phenomenon caused by environmental sources [32].

Figure 3.14: The K Sonar Cane. Source: [45]

CHAPTER 4

Acoustic techniques for direct coupling's reduction

The aim of this thesis is to find a solution to the acoustic coupling which exists between the ultrasound transmitter and receiver. To address this problem there are two viable options: simulation and 3D printing. Problem-solving through software development includes a set of activities such as requirements analysis, software implementation followed by testing and validation. On the other hand, 3D printing starts with the establishment of the prototype functionality, being succeeded by the development and evaluation phases. In the evaluation phase, the prototype is used and tested to find out if the 3D piece meets all the requirements specified initially. If issues are detected, the feedback obtained previously is used to improve and adjust the new prototype. Among the two options, 3D printing was chosen since the degree of complexity to develop an algorithm capable of reducing the acoustic coupling is too high when compared to the use of mechanical techniques.

This technology makes it possible to transpose a concept or an idea to a physical object in a short period of time. 3D printing also enables total customization of the prototype including the design of complex geometric shapes that are extremely complicated and expensive to produce using traditional means.

This process initiates using a modeling software Computer Aided Design (CAD) in which the geometry of the model is defined in 3D. The model is then converted into a STL format which defines the geometry of the 3D object translating the initial design into a readable file for the 3D printer. After this step, this file is transferred to the 3D printer. The printers utilized during this dissertation were the Beethefirst and BeenInSchool which uses the Fused Deposition Modeling technology. This technique, also known as FDM, selectively deposits plastic filament in a pre-determined path layer-by-layer to construct the drawn object. Once the printing process is finished, the 3D piece is removed from the printer's platform and may need some final touches such as polishing or sanding.

In the context of this master thesis, 3D printing was used to produce several supports for the ultrasound transducers with different shapes and formats, in order to reduce the acoustic coupling. Based on the results and conclusions drawn with each prototype during the evaluation phase, it was possible to obtain a final 3D piece where this negative effect was greatly reduced.

4.1 TESTING SYSTEM

To test each one of the 3D supports designed, it was assembled a test system in which all supports could be tested under the same conditions. The implemented system enabled not only to send and acquire ultrasounds but also to store all the reflected echoes into *.wav* files so these could be later analyzed using MATLAB.

Therefore, in a first approach, it will be presented all the software and hardware resources from the test system as well as their functions and features. This includes a detailed description of how to record and capture ultrasounds using the Roland audio card. Even before presenting the first 3D support drawn, in section 4.1.2 is explained the operation principle of the test system as wells as an elaborated description of the tests performed to the 3D supports.

4.1.1 SOFTWARE AND HARWARE USED

4.1.1.1 MATLAB

MATLAB stands for MATrix LABoratory and it is a highly sophisticated numerical calculation tool developed by The MathWorks, Inc. One of its strengths comes from combining computing, visualization, and programming in a simple-to-use environment. Matlab has become a standard tool in engineering and science because complex numerical problems can be solved easily in a fraction of time required with programming languages like Fortran or C.

In a first approach, MATLAB was used to generate the *wav* file containing the pulses meant to drive the transmitter transducer. To start with, 400 periods of a sinusoid with a frequency of 40kHz and duration of 10 milliseconds were generated. The time between each burst was 100 miliseconds. Afterwards, using the audiowrite routine it was created a wav file containing the generated signal. The total duration of this audio file was 11 seconds and it was named as 'TestSignal.wav'.

Lastly, after performing the tests with each one of the 3D supports, this tool was used to calculate the maximum amplitude of the recorded signal, the value of the variance, as well as, for graphical visualization of the received signals.

4.1.1.2 AUDACITY

Audacity is a free, open-source software used for editing and recording audio, being available on Windows, Mac OS X, GNU/Linux, and other operating systems.

This software allows the user to import and export various audio formats such as wav and mp3 and its project rate can go up to 384000 Hz. In this context, this program was used to reproduce the wav file *TestSignal* which contained the pulses to be transmitted by the emitter transducer and, to record the reflected echoes acquired by the receiver transducer.

4.1.1.3 AUTODESK FUSION 360

Autodesk® Fusion 360 is a clouded-based produt development platform which combines CAD, CAM and CAE into one integrated workflow. It is a multi-discipline tool since it incorporates industrial

design, mechanical engineering, and machine tool programming. Fusion 360 it is often used for 3D printing projects and it runs on Windows, Mac and in web browsers.

In this specific case, this software was used throughout the whole master thesis to design all 3D models, more specifically, the transducers supports.

4.1.1.4 TRANSDUCERS

The ultrasonic transducers chosen were the MA40S4T/R from Murata since they present a good compromise between cost, size, and reliability. Both transducers have a nominal frequency of *40 kHz* and their dimensions are displayed in figure 4.1(b). Looking at this figure, it is possible to verify that the diameter of each transducer corresponds to 9.9 *mm*. This particular information was necessary to design the various supports.

The figures 4.1(c) and 4.1(d) show the radiation diagrams of both sensors. Throught its analysis, it is possible to state that for $\theta = 0°$ the transducers have their maximum value which is attenuated as the angle opens. According to the manufacturer's data, both transducers have a typical directivity of 80°.

(a) MA40S4S/R Murata transducers

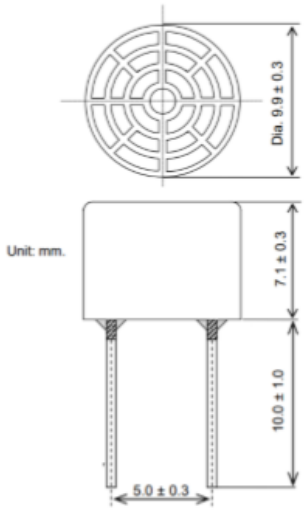

(b) Transducer dimensions

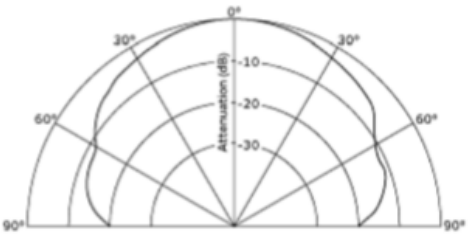

(c) MA40S4S radiation diagram

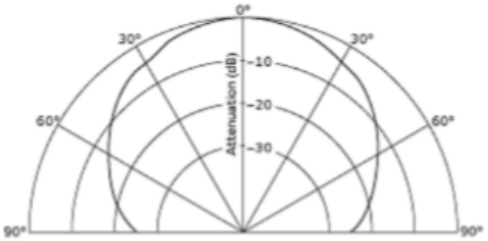

(d) MA40S4R radiation diagram

Figure 4.1: MA40S4S/R Murata transducer.

4.1.1.5 SOUND CARD ROLAND - QUAD-CAPTURE

The QUAD-CAPTURE is a sound card from Roland with two Ground Left Right (XLR) inputs, two Tip Ring Sleeve (TRS) inputs, two TRS outputs, headphone output and it is Universal Serial Bus(USB) bus powered. This USB connection in addition to powering the sound card also allows the exchange of data with the computer. Furthermore, this device is capable of delivering high sound quality with recording and playback rates up to 24-bit/192kHz. Also, the two inputs have microphone preamps which can be digitally configurated through the graphical Quad-Capture Control Panel software. Before connecting the sound card to the computer for the first time, it was necessary to install the QUAD-CAPTURE device driver software and to make some adjustments in the sound settings to be possible the recording of ultrasounds. Firstly, the QUAD-CAPTURE control panel was accessed through the Windows sound settings and the toolbar *Driver* was selected as shown in figure 4.2. Nextly, a window with the *QUAD-CAPTURE Driver Settings* was displayed and the sample rate of 192000Hz was chosen.

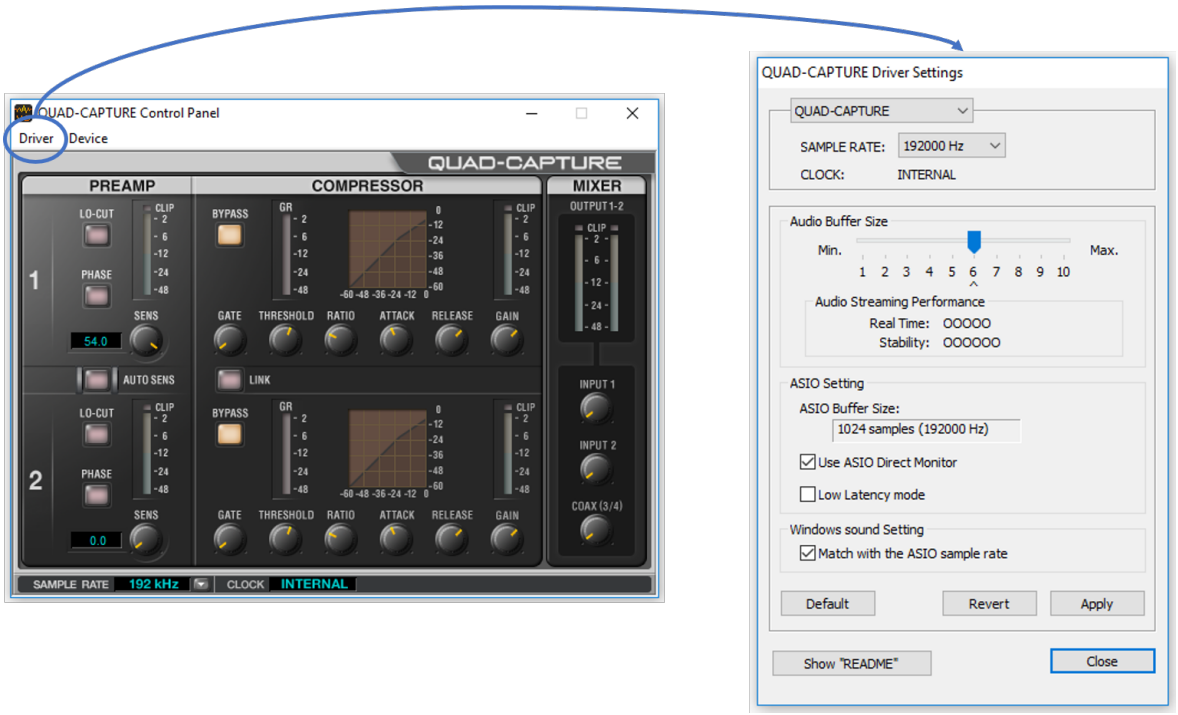

Figure 4.2: First step to setting up the sound card to record ultrasounds.

Moreover, it was also required to ensure that the previously selected sampling rate also appeared in the *Sound settings* of the Windows control panel. After accessing this panel, the navigation steps were: Hardware and Sound > Sound > Recording > 1-2 QUAD-CAPTURE > Properties > Advanced. Afterwards, in the *Default Format* the chosen option should be *'2 channel, 24 bit, 192000 Hz (Studio Quality)'* as shown in the figure 4.3.

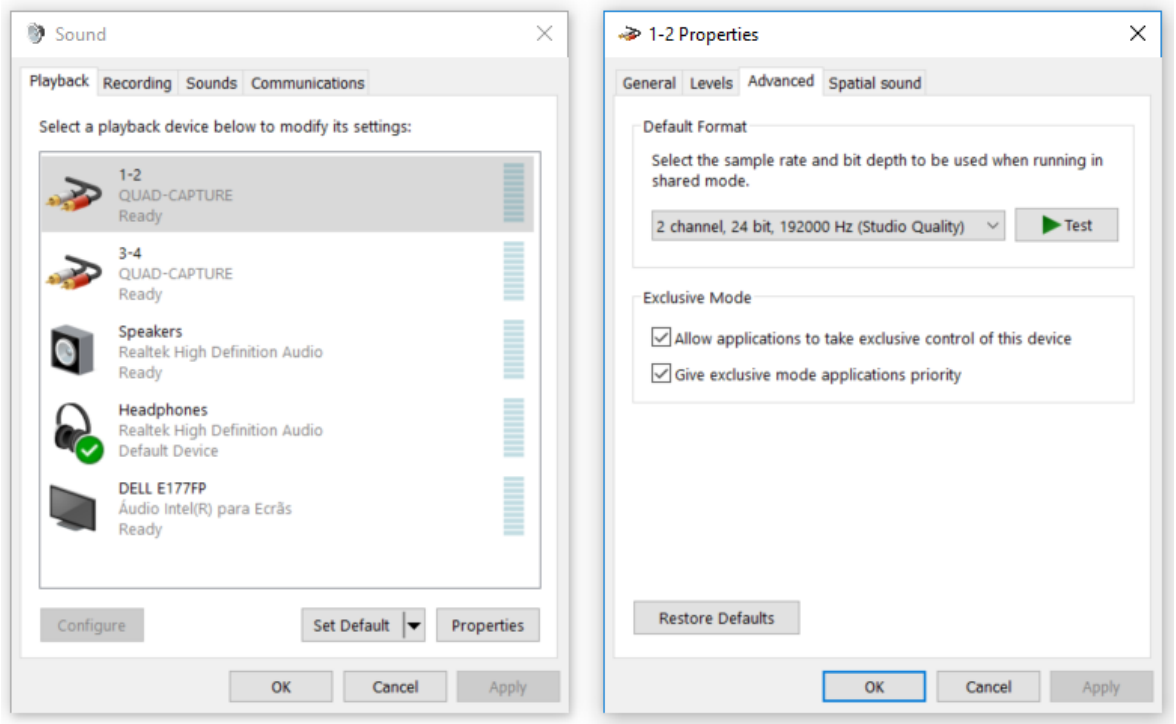

Figure 4.3: Second step to setting up the sound card to record ultrasounds.

As previously mentioned, this device has two XLR inputs named as input 1L and input 2R (figure 4.4). Since only one input was needed and following the recommendations of the instructions manual the input 1L was used to connect the receiver transducer. The potentiometer was placed in the playback position to guarantee that there wasn't any feedback, ie the sound card did not reproduce the input signal along with the output signal.

Figure 4.4: Front view of the sound card.

Regarding the back side of the audio interface, the switches PHANTOM, NOR and GROUND LIFT were set to the off position as shown in figure 4.5. The settings mentioned in this subsection relatively to the sound card configuration were maintained throughout the entire project.

Figure 4.5: Back view of the sound card.

4.1.2 OPERATION OF THE TEST SYSTEM

The figure 4.6 presents the block diagram of the platform of tests implemented which include the Roland sound card, two ultrasonic transducers, a portable computer and the target. The target refers to the surface used to reflect the ultrasound waves. In this case, the white board present in the laboratory was utilized due to its good reflection properties.

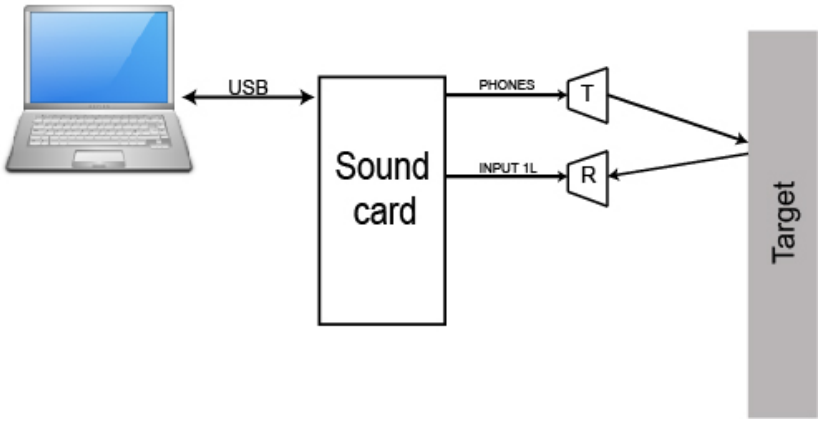

Figure 4.6: Setup used.

Before testing any of the printed 3D pieces, it was necessary to connect the computer and the ultrasound transducers to the sound card and check if all settings are as described in section 4.1.1.5.

Afterwards, to guarantee that all supports are evaluated under the same conditions some measures were taken. Firstly, to fix the several 3D supports containing the ultrasound transducers, it was used a metal tube where these pieces could be easily placed and removed. Nextly, to assure that these were always at the same distance and height from the target, the metal tube was permanently attached to a microphone stand that was available in the laboratory and placed at two meters from the white board.

In order to evaluate the performance of each one of the 3D models designed, and according to the origin of the acoustic coupling to be measured, two types of tests were performed.

The first test that was performed on all 3D supports and includes the following steps:

- **Step 1** The file *TestSignal.wav* generated by *Matlab* and whose characteristics were described in section 4.1.1.1 is imported to *Audacity*.
- **Step 2** This file is played and sent to the transmitting transducer through the sound card. Consequently, the receiver transducer acquires the echoes reflected by the obstacle which are processed by the computer.
- **Step 3** The audio track containing the reflected echoes is then exported and saved into a wav file.
- **Step 4** Using the *audioread* routine of *Matlab*, the samples of the recorded signal are obtained. Afterwards, the module of the maximum value recorded as well as the variance are calculated.

The second test was only performed at a later stage in the design of the supports. The difference between this test and the first one is that in the second step while the wav file was played, the hole of the 3D support corresponding to the emitter transducer was covered with the index finger.

4.2 3D SUPPORTS DESIGNED TO REDUCE THE ACOUSTIC COUPLING

In this section, all the different prototypes produced to reduce the effect of the acoustic coupling are presented. This work began with the design of a simple prototype named as version 1. This 3D part allowed to verify the existence of the acoustic coupling in the worst case scenario, that is, when there wasn't a physical barrier that prevented the signal from passing directly from the transmitter to the receiver. This prototype went through several modifications throughout the different versions of the 3D supports until reaching a final product. At the end of each version are presented the obtained results as wells as the conclusions drawn.

4.2.1 VERSION 1

For the first version of the 3D supports, it was designed a very simple 3D support where the two ultrasonic transducers could be placed side by side. As shown in figure 4.7, this 3D model also contained a structure with a cylindrical shape that allowed the fitting of the transducer support into the metal tube from the test system.

The holes 1 and 2 correspond to the places where the receiver and the transmitter transducers were placed accordingly. Each one of the orifices designed in the support had a diameter of *10 mm* to ensure a snug fit of the transducers.

Figure 4.7: 3D model of the first support.

The result of the first 3D model printed is shown in figure 4.8. Nextly, this piece was placed into the metal tube and the transducers were properly placed in the orifices. The positioning of the transducers was maintained for the remaining 3D pieces, that is, in the upper part of the support it was always placed the emitter transducer and in the lower part the receiver transducer.

In figure 4.9 it is possible to visualize the finished setup.

Figure 4.8: First 3D support printed.

Figure 4.9: Setup used to test the first version of the transducer support.

4.2.1.1 OBTAINED RESULTS

The version 1 was tested following the first test steps described in section 4.1.2. Observing the figure 4.10 that contains the first pulse sent and the respective recorded signals is quite visible the presence of acoustic coupling. This has a maximum amplitude of 0.3356, which is approximately 14 times bigger than the echo reflected by the surface. As stated in the section 2.4, since the acoustic coupling does not have an amplitude lower than the reflected echo, it can be interpreted as being one causing an incorrect detection of obstacles or measurement of distances.

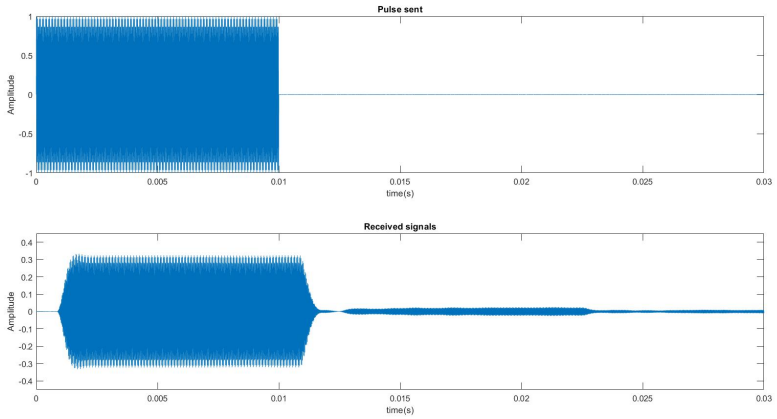

Figure 4.10: First pulse sent and received signals using the 1st version of the 3D support.

$\max\|RecordedSignal\|$
0.3356

Table 4.1: Maximum value in modulus of the recorded audio signal from version 1.

For *40kHz* and considering that the velocity of the sound is about *344 m/s*, for a distance of two meters the echo must be received after *11.7 milliseconds*.

Using the *ginput* function from MATLAB, the points corresponding to the initial and final instants of the acoustic coupling and echo were identified. This allowed to calculate the duration of each signal, the acoustic coupling initiates at *t=1.1 milliseconds* and ends at *t=11.1 milliseconds* having a total duration of *10 milliseconds*. On the other side, the echo was received at *t=12.7 milliseconds* and ends approximately at *t=22.7 milliseconds* also having a duration of *10 milliseconds*. The small delay is caused by the sound card latency which does not have a fixed value. The variation of this delay is due to the different processing times that the computer and the sound card take.

4.2.2 VERSION 2

In the second support designed, also called as, version 2 the focus was towards the acoustic coupling through the air $H_3(s)$. For that purpose, two aluminum tubes with an internal diameter equal to the diameter of the transducers were used to prevent the signal being sent by the emitter transducer to be detected by the receiver. This tubes were used to change the radiation diagram of both transducers so the radiated field at 90° would be zero.

In this version, the only change made regarding the first one was the increase of the diameter of the holes from *10mm* to *13.5mm* to allow the aluminium tubes to be placed in the support.

Figure 4.11: 3D model of the second version and printed piece(respectively).

To test this version, two different parameters were changed: *d1* which corresponds to the position of the transducer inside the aluminum tube and *d2* which consists of the length of the tube outside the front part of the 3D support 4.12. Regarding the *d2* parameter, tests were carried out for 4 different lengths: 0 *cm*, 0.5 *cm*, 1*cm* and 2*cm*. For both parameters, *d1* and *d2*, it was performed the first test described in section 4.1.2.

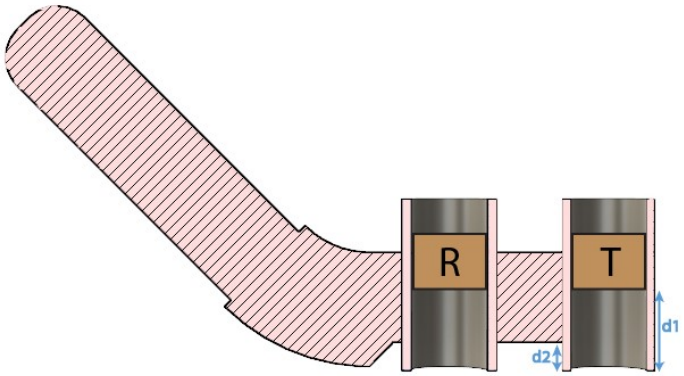

Figure 4.12: Mid plane of the second version with respective measures.

4.2.2.1 OBTAINED RESULTS

In table 4.2 are present the results obtained with this version for the different values of *d1* and *d2*. Comparing the maximum values in module of the recorded signals with the value of 0.3356 from the first version, it is possible to verify that there was an overall improvement.

	$d_2(cm)$	$d1(cm)$	max$\lvert RecordedSignal \rvert$
Version 2	0	0	0.3370
		1	0.3071
		2	0.164
		3	0.1419
	0.5	0	0.1381
		1	0.1120
		2	0.0917
		3	0.0956
	1	0	0.1963
		1	0.0499
		2	0.1612
		3	0.1169
	2	0	0.1511
		1	0.1450
		2	0.1096
		3	0.0740

Table 4.2: Variance and maximum value in modulus of the recorded audio signal from version 2.

The figure 4.13 shows an emitted pulse and the respective received signals when *d1 = 1cm* and *d2 = 1 cm* which corresponds to the best result obtained with this version. Through its analysis, it is notorious that the amplitude of the acoustic coupling decreased significantly comparatively to the same figure from the first version(figure 4.10). It is also possible to verify that the amplitude of the acoustic coupling is approximately of the same order of the magnitude of the reflected echo which did not happen in the latest version.

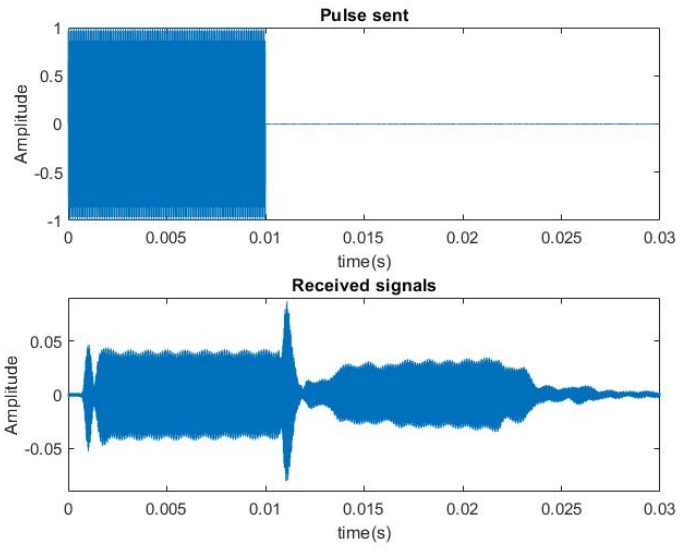

Figure 4.13: First pulse sent and received signals using the 2nd version of the 3D support.

4.2.3 VERSIONS 3 AND 4

For the thirds and fourth versions, the aim was to further reduce the effect of $H_3(s)$ by combining the aluminium tubes used in the second version with acoustic barriers in the middle of the supports.

At structural level, in these new versions additional supports for the metal tubes were included since it was verified in the previous version that these were not totally fixed in the 3D piece.

In version 3, in addition to the supports, different pyramids of sponge were cut and later glued between the two transducers (figure. 4.14). These sponge pyramids were inspired by the acoustic foam panels often used in studios and movie theaters for sound absorption due to their porous surface. In this version, the purpose of these pyramids was the creation of multiple paths that the ultrasounds would have to go through and in which their energy would dissipate.

On the other hand, in version 4, the small pyramids of different heights and angles of rotation were designed directly in the 3D model between the two orificies(figure. 4.15). In this case, the pyramids were thought to be a random labyrinth where the ultrasounds would undergo multiple reflections.

The performance of the two 3D pieces were evaluated using once again the first test with the nuance that in version 4 the maximum value of *d2* used was *0.5 cm* since this was the maximum height of the pyramids.

Figure 4.14: 3D model of the third version and printed part (respectively).

Figure 4.15: 3D model of the forth version and printed part (respectively).

4.2.3.1 OBTAINED RESULTS

The following tables 4.3 and 4.4 present the obtained results for versions 3 and 4 respectively.

	$d_2(cm)$	$d_1(cm)$	$\max\|RecordedSignal\|$
Version 3	0	0	0.0934
		1	0.0817
		2	0.0871
		3	0.0702
	0.5	0	0.1150
		1	0.1563
		2	0.1134
		3	0.0382
	1	0	0.1454
		1	0.1174
		2	0.1674
		3	0.0583
	2	0	0.2061
		1	0.1532
		2	0.1436
		3	0.6670

Table 4.3: Maximum value in modulus of the recorded audio signal from version 3.

	$d_2(cm)$	$d_1(cm)$	$\max\|RecordedSignal\|$
Version 4	0	0	0.3196
		1	0.1841
		2	0.2437
		3	0.1586
	0.5	0	0.0934
		1	0.0934
		2	0.0518
		3	0.0884

Table 4.4: Maximum value in modulus of the recorded audio signal from version 4.

Analyzing both tables it is possible to verify that in versions 3 and 4 lower values were obtained relatively to those acquired in the previous versions with special emphasis on the version 3 which had the best result of all the four versions for *d2 = 0.5 cm* and *d1 = 3 cm*.

The results obtained with version 3 are related to the use of the sponge as this prevents the ultrasound from traveling from the emitter to the receiver. Since it is a porous material, part of its volume is constituted by small air cavities communicating with each other and with the exterior. During signal transmission, the ultrasounds penetrate the pores and are then reflected several times while dissipating their energy.

Regarding the version 4, it was verified that the best results were acquired for *d2 = 0.5 cm* and *d1 = 2 cm*. The material used to print this 3D piece, as well as, the remaining pieces was 3D

printing filament. It is, therefore, a dense material which was used to create several barriers to prevent ultrasound from spreading to the receiver.

4.2.4 VERSION 5

In this version of the 3D support, it was applied the Huygens' principle along with the Fourier transform to calculate the diameter of an apperture which produced a field strenght of zero in the direction of the receiver transducer. In this way, $H_3(s)$ would be eliminated. Nextly are presented all the calculations and approximations performed to achieve the value of the apperture, starting with a short description of the phenomenon of the diffraction of light.

4.2.4.1 HUYGENS' PRINCIPLE AND APPLICATION OF THE FOURIER TRANSFORM

One of the most important phenomenons associated with the theory of light is diffraction which can be defined as the ability of the light waves to bend around an obstacle or apperture . As a plane light wave passes through a slit in a opaque barrier it spreads out in all forward directions[46]. This phenomenon occurs with all waves including sound waves, water waves and electromagnetic waves[47].

For this case, light was considered an electromagnetic wave with the following properties:

- Monochromatic: which means that the periodicity in time is a single frequency;
- Linearly polarized: which means that the electric field and magnetic vectors stay in a plane as the light wave moves.

Based on the characteristics presented previously it is possible to describe the wave light through a scalar-valued function of time and position. This function is the magnitude of the electric field and has the following form (4.1)

$$F(x)cos[wt - \phi(x)] \tag{4.1}$$

where *F(x)* is the amplitude as a function of the position in space, w is the angular frequency, and $\phi(x)$ is the phase in space. In this case, it is helpful to use the phasor notation. Thus, the phasor *E(x)* is given by (4.2)

$$E(x) = F(x)e^{-i\phi(x)} \tag{4.2}$$

Then, the time-dependent function *E(x,t)* is equal to (4.3)

$$E(x,t) = Re[E(x)e^{iwt}] \tag{4.3}$$

The equations above are related to one single source. Considering now an infinite plane with infinite sources it is possible to calculate the electric field, in this case, using the Huygens' principle by summing up the effects of all of the sources at a given point P.

Thus, the field at a point P at a distance r (figure 4.16) due to an element between x and $x + dx$ is proportional to (4.4)

$$E(x)dxe^{-2\pi r/\lambda} \tag{4.4}$$

where the phase shift $2\pi r/\lambda$ refers to the number of wavelengths that are necessary to go throught the distance r. By looking at the figure 4.16, the distance r can be defined as (4.5)

$$\begin{aligned} r &= R + xsin\theta \\ &= R + xs \end{aligned} \tag{4.5}$$

where θ is the angle between the z-axis and the point P, and s=$sin\ \theta$. By substituing this r value in the equation (4.4) it is obtained the following equation

$$E(x)dxe^{\frac{-2\pi}{\lambda}(R+xs)} = E(x)e^{-i2\pi R/\lambda}e^{-i2\pi xs/\lambda}dx \tag{4.6}$$

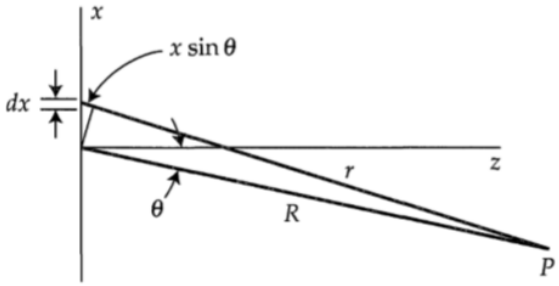

Figure 4.16: Geometric construction for applying Huyghens'principle. Source:[48]

Thus, the total field at P can be calculated by integrating the previous equation 4.6, and by droping out the constant $E(x)\ e^{-i2\pi R/\lambda}$ since it is not important for the remaining considerations. Therefore, the total field is given by

$$\int_{-\infty}^{\infty} E(x)e^{-i2\pi xs/\lambda}dx \tag{4.7}$$

For convenience, the previous equation 4.7 was normalized in terms of the wavelength λ. Thus, $P(S)$ which is defined as the field radiation pattern or angular spectrum can now be described by the following equation (4.8):

$$P(s) = \int_{-\infty}^{\infty} E(\frac{x}{\lambda})e^{-i2\pi xs/\lambda}d(\frac{x}{\lambda}) \tag{4.8}$$

A Fourier transform relation exists between the w_λ and the correspondent raddiation pattern. A rectangular pulse with a width of w_λ is analogous to $E(\frac{x}{\lambda})$. Moreover, the definition of Fourier transform can be described by the equation (4.9):

$$\mathcal{F}(w) = \frac{1}{\sqrt{2\pi}}\int_{-\infty}^{\infty} f(t)e^{-iwt}dt \tag{4.9}$$

and the inverse Fourier transform is given by (4.10):

$$f(t) = \frac{1}{\sqrt{2\pi}}\int_{-\infty}^{\infty} \mathcal{F}(w)e^{itw}dw \tag{4.10}$$

Considering that the time t corresponds to the normalization of x that is $(x/\ \lambda)$ and the frequency f corresponds to the s it follows that 4.11:

$$E(\frac{x}{\lambda}) = \int_{-\infty}^{\infty} P(s)e^{i2\pi(x/\lambda)s}d(s) \tag{4.11}$$

Also, the Fourier transform of a rectangular function is the *sinc* function (figure 4.17). Thus,

$$P(s) = w_\lambda sinc w_\lambda s \tag{4.12}$$

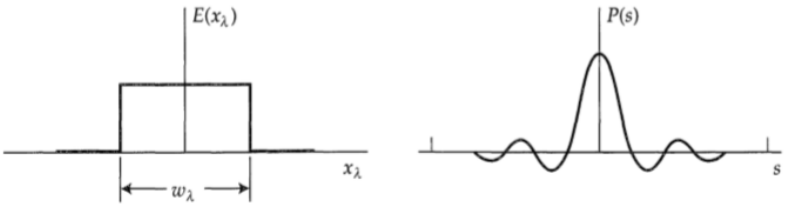

Figure 4.17: Apperture distribution and its respective angular spectrum. Source:[48]

Having this said, the field P is the Fourier transform of the radiant field E.

Analyzing figure 4.18 it is possible to verify that the ultrasound transducer also creates a field similar to a rectangular function. By analogy, it is possible to conclude that the field created by the transducer is also the function sinc. Thus, a possible solution to eliminate the acoustic coupling through the air ($H_3(s)$) might be to modify the radiation diagram from the emitter transducer. Therefore, the field strenght of the emitter transducer in the direction of the receiver transducer must be zero. This is achieved when the angle θ is equal to $\pi/2$.

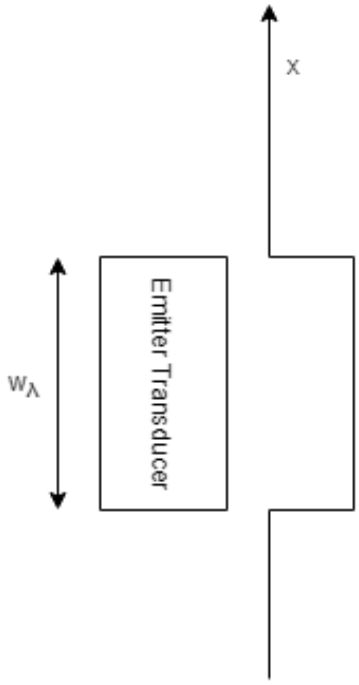

Figure 4.18: Radiation pattern of the ultrasonic transducer in function of w_λ.

When observing the equation 4.12 relative to the field radiation pattern it is possible to verify the existence of the *sinc* function which by definition is equal to (4.13):

$$sinc(x) = \frac{sin(\pi x)}{\pi x} \tag{4.13}$$

Substituing this expression 4.13 into equation 4.12 results in (4.14)

$$P(s) = w_\lambda \frac{sin(\pi s w_\lambda)}{\pi s w_\lambda} \tag{4.14}$$

Since the main goal is to have a zero when $\theta = \pi\ /2$, the previous equation 4.14 was set to zero. Therefore, that equation becomes

$$sin(\pi s w_\lambda) = 0 \tag{4.15}$$

The condition $sin\theta$=0 is verified when $\theta\ = k\pi$. Thus

$$\pi s w_\lambda = k\pi \Leftrightarrow s w_\lambda = k \tag{4.16}$$

The first zero of $sin\theta$ is defined for k=*1* resulting on

$$s = \frac{1}{w_\lambda} \tag{4.17}$$

Since the $sin\theta$ in $\pi\ /2$ is equal to 1, w_λ is equal to

$$w_\lambda = 1 \Leftrightarrow \frac{w}{\lambda} = 1 \Leftrightarrow w = \lambda = \frac{c}{f} = \frac{343m/s}{40000Hz} = 8.575mm \tag{4.18}$$

4.2.4.2 FIFTH SUPPORT

In view of the above, it was drawn the transducers support from version 5. In comparison to the previous models 3 and 4, the diameter of the holes in the support were reduced to *10mm* since the metal tubes would not be used. However, the previous calculations have shown that an aperture of *8.575 mm* results on a emitted radiation to the receiver transducer of zero.

Therefore, the strategy used was to extend and taper the supports of the transducers from *10mm* to *8.575mm*. This originated two additional structures in front of each transducer with the shape of a truncated cone as shown in figure 4.19.

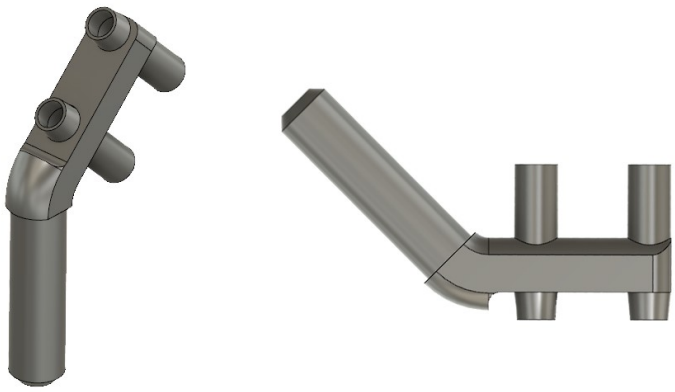

Figure 4.19: 3D model of the fifth version.

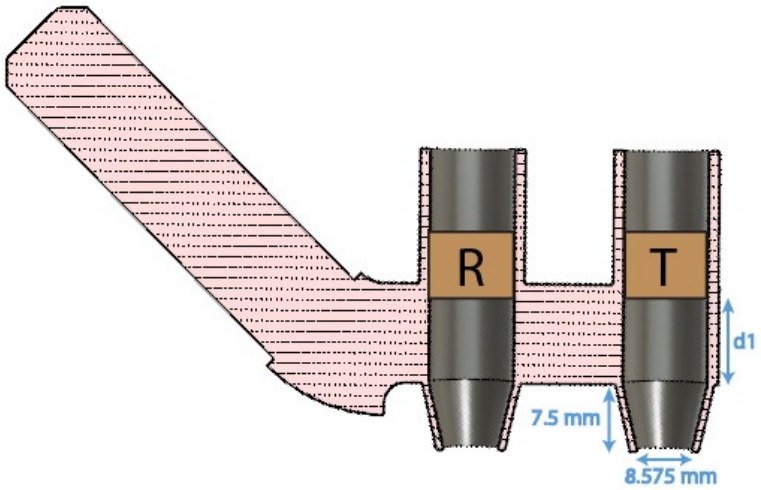

Figure 4.20: Mid plane of the fifth version.

After printing the 3D model, it was initiated the evalution phase. In this case, both tests described in section 4.1.2 were performed.

After performing both tests, it was glued a single piece of upholster foam between the two truncated cones of the support and both tests were repeated (figure. 4.22). In this case, the aim was to verify if this material would once again decrease the impact of $H_3(s)$.

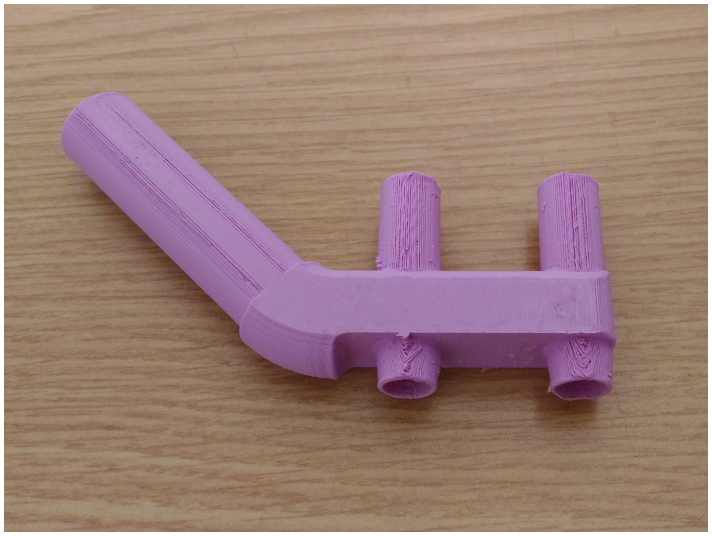

Figure 4.21: Printed part of the fifth version.

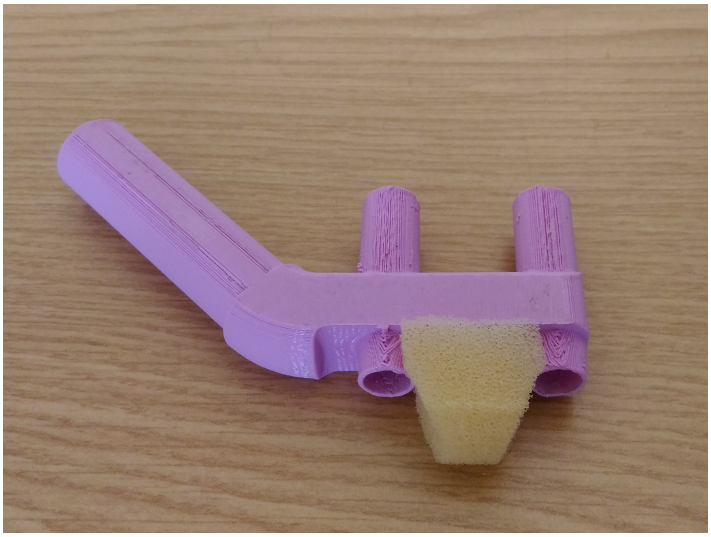

Figure 4.22: Printed part of the fifth version with upholster foam between the emitter and receiver truncated cones.

4.2.4.3 OBTAINED RESULTS

Observing both tables 4.5 and 4.6 which contain the results obtained for the support with and without the upholster foam, it is possible to verify a general improvement of the results compared to those obtained with the previous versions. The effect of $H_3(s)$ was significantly reduced considering that in the versions 3 and 4 the lowest values obtained were *0.0382* and *0.0518* and the highest were *0.6670* and *0.3196* respectively. However, it is visible a large discrepancy between the highest and lowest values obtained in both versions. On the contrary, in this version thanks to the use of the truncated cones, the smaller and higher results acquired are all in the same range of values and, there aren't any major fluctuations between the different values. The smallest value of the maximum modulus of the recorded signal was acquired using the foam version which corresponds to 0.0397 for d_1 = 0.75 *cm*. This is in agreement with the conclusions drawn in version 3, that is, the sponge plays a fundamental role in the reduction of $H_3(s)$ since, thanks to its structure, it allows the ultrasounds to penetrate through its material being at the same time attenuated.

	$d_1(cm)$	$\max\lvert RecordedSignal\rvert$
Version 5 without upholster foam	0.75	0.0621
	0.85	0.0512
	0.95	0.0703
	1.05	0.0739
	1.15	0.0768
	1.25	0.0736

Table 4.5: Maximum value in modulus of the recorded signal in the 5th version without upholster foam.

	$d_1(cm)$	$\max\|RecordedSignal\|$
Version 5 with upholster foam	0.75	0.0397
	0.85	0.0443
	0.95	0.0398
	1.05	0.0476
	1.15	0.0551
	1.25	0.0427

Table 4.6: Maximum value in modulus of the recorded signal in the 5th version with upholster foam.

Regarding the second test performed in both cases, when the emitter was tapped the receiver continued to detect signal. Thus, it is possible to infer that the emitter is not acoustically isolated from the receiver. Ideally, when the truncated cone from the transmitter was covered up, the ultrasound source would be eliminated and therefore no ultrasound should be acquired by the receiver. This test confirms that the ultrasounds propagates not only by the air but also by other paths as described in section 2.4.

4.2.5 INDIVIDUAL SUPPORTS

After the conclusions drawn from version 5, it was necessary to understand with more detail which other mediums were used by the ultrasounds to reach the receiver. One possible hypothesis would be that the signal was propagating through the plastic structure of the supports. Therefore, two individual supports were created for each one of the transducers based on the truncated cones used in the version 5. These are shown in figure 4.23 and their dimensions are present in the figure 4.24.

Figure 4.23: 3D model of the individual supports and printed parts (respectively).

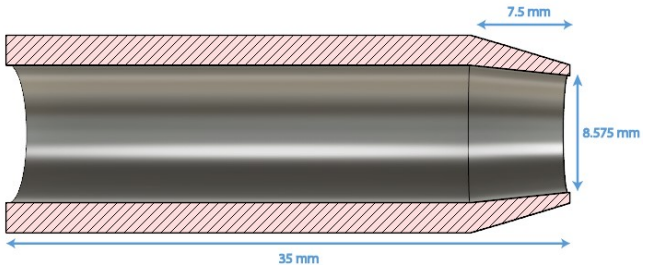

Figure 4.24: Mid plane of the individual supports.

These supports were meant to take out of the equation $H_1(s)$ and $H_2(s)$ and verify in this context if the only pathway that remained was $H_3(s)$.

To ensure that $H_1(s)$ and $H_2(s)$ were in fact fully erased two measures were taken. Firstly, the back of both supports was covered up with sponge thus removing $H_1(s)$ from the panorama. Secondly, to guarantee that there was no physical connection between both transducers, the receiver transducer was attached to the microphone holder used previously. Regarding the emitter transducer, it was attached to a wooden stand from the laboratory (figure. 4.25). The height of both stands was adjusted to maintain the emitter and receiver configuration used in the other tests, i.e., the emitter transducer was placed at a slightly higher height relative to the receiver (figure. 4.26). Special attention was taken so there was no physical contact between the two stands used.

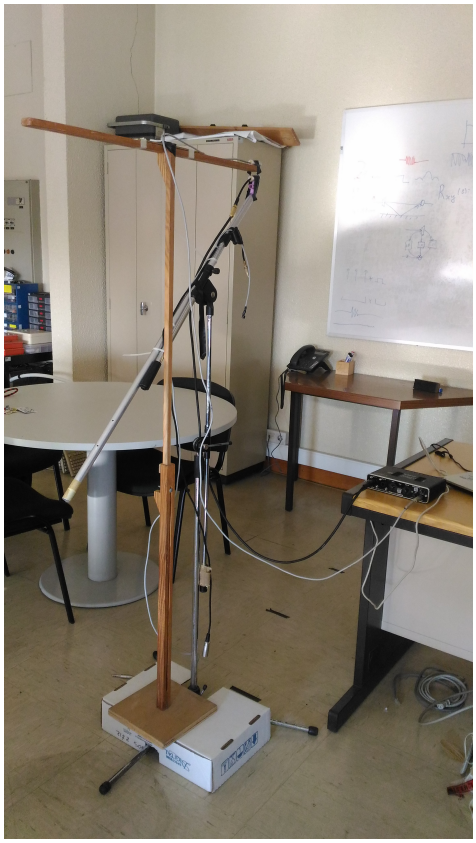

Figure 4.25: Setup used to test the individual supports.

Figure 4.26: Positioning of the individual supports in the stands.

4.2.5.1 OBTAINED RESULTS

After the setup described in the previous section 4.2.5 was completed, the individual supports were tested. To test these supports both tests described in section 4.1.2 were executed. In the first test the transducer was colocated at a distance *d1* of *0.75 cm* and it was obtained a maximum value in modulus of the recorded signal of *0.0442*. Since the effects of $H_1(s)$ and $H_2(s)$ were eliminated, this value of the acoustic coupling is only related to $H_3(s)$. For the same distance, in the fifth support without the upholster foam it was obtained a value of *0.0621*. Comparing both values it is possible to conclude that $H_2(s)$ has a major contribution on the total value of the acoustic coupling.

Regarding the second test performed, the emitter transducer was capped and contrary to what succeded in version 5, it was verified that the receiver transducer could not detect any ultrasound signal. With this result it was concluded that ideally both the transmitter and the receiver transducer should not share the same material between them in order to avoid the propagation of the ultrasound through the 3D sctructure which causes $H_2(s)$.

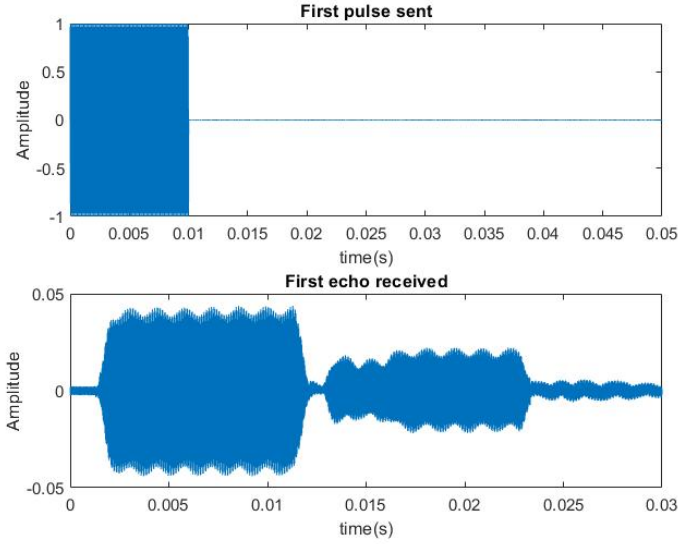

Figure 4.27: First pulse sent and received signals using the individual supports of the transducers.

$\max\lvert RecordedSignal\rvert$
0.0442

Table 4.7: Maximum value in modulus of the recorded audio signal of the individual supports.

4.2.6 VERSION 6

All things considered, a new support for the transducers, named as version 6, was created. The projection of the new version was a junction of two different concepts:

- The truncated cones which were previously utilized in version 5 and for the individuals supports due to their capability to reduce the acoustic coupling through the air;
- The use of a spongy material between the two transducers to prevent the ultrasounds to travel mechanically from the emitter to the receiver

Following that idea, this version combined two different supports which were built separately, the main support (figure. 4.28a) as well as the individual supports(figure. 4.28b).The figure 4.28 shows the dimensions of the two 3D pieces designed.

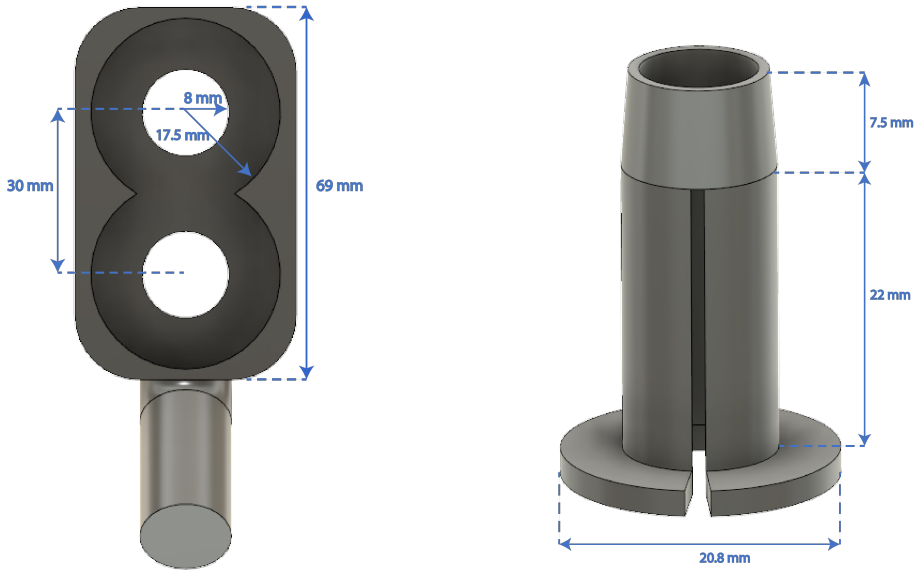

(a) Dimensions of the main support

(b) Dimensions of the individual support

Figure 4.28: 3D models of the two 3D supports of the version 6 and their dimensions.

The interior of the main support (figure. 4.28a) has a cavity in the shape of the number eight as it allows to evenly place insulation material between the two transducers. In addition, it also provides a better stability for both transducers. The two circumferences existing in the main support were designed with a radius large enough so that after placing the insulation material around the individual supports these do not touch the main structure. Thus, transmission of the signal from the transmitter to the receiver through the main support is avoided.

Concerning the individual support, a flange was added to the base of the support for two reasons. In the first place, the flange allows a greater attachment of the individual support to the spongy material. Additionally, it ensures that after the assembly of the version 6 is completed as shown in figure 4.31, both individual supports are positioned equally inside the main support. Furthermore, a groove was created in the lateral of the support to facilitate the placement of the transducer therein. The internal diameter of the supports was defined as $10mm$ so that both transducers are steady and fixed.

The figures 4.29 and 4.30 show the result of the 3D printing of the main structure and the individual supports respectively.

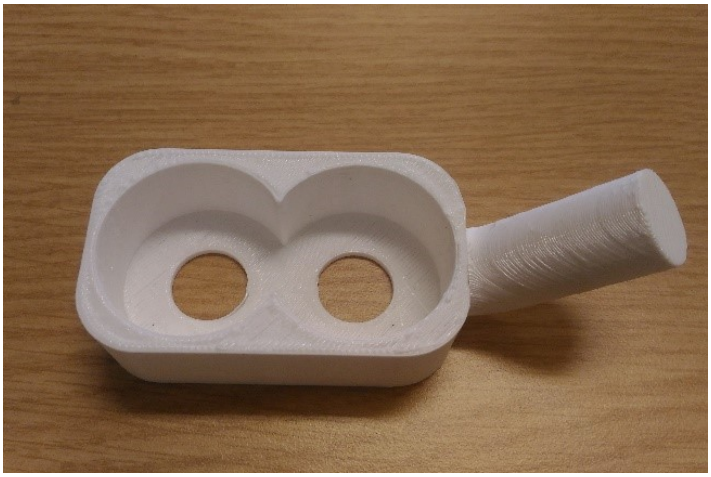

Figure 4.29: Main support of the 6th version.

Figure 4.30: Individual supports of the 6th version.

In figure 4.31 it is possible to see the complete assembly of the version 6 with the different supports along with the insulation material.

In relation to the insulation material, a spongy material was chosen more specifically, the elastomeric foam. This foam is frequently used for both thermal and acoustic insulation and it applied in cold-heat pumps, ducts, cooling systems and noise attenuatuon between floors. When it comes to acoustic insulation this foam has a great performance thanks to its open cell structure with a complex geometry of the pores guaranteeing an effective sound absorption. On the other hand, its high density results in a powerful reduction in the propagation of sound.

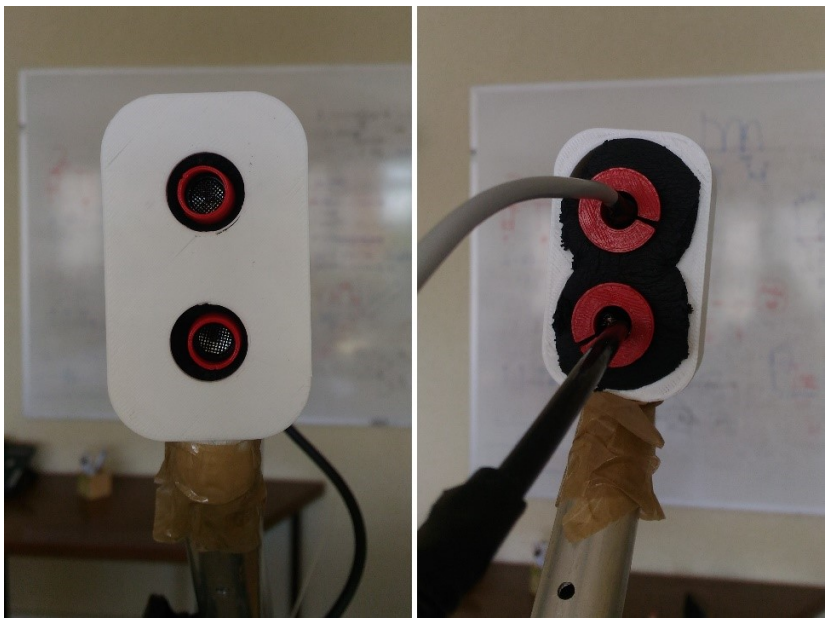

Figure 4.31: Assembly of the sixth version.

4.2.6.1 OBTAINED RESULTS

To evaluate the performance of this version the initial microphone holder was used and the procedure described in 4.1.2 repeated. The obtained results are shown in the table 4.8.

Through its analysis, it is possible to affirm that with this support it was obtained the best result in terms of the maximum value of the recorded signal in module as well as the variance in comparison to the other supports designed. Observing the figure 4.32 it is still visible the presence of the acoustic coupling along with the echo received. Even so, it is notorious the progress made since the first 3D support in which the amplitude of the acoustic coupling was approximately 0.3356.

$\max\lvert RecordedSignal\rvert$
0.0120

Table 4.8: Maximum value in modulus of the recorded audio signal.

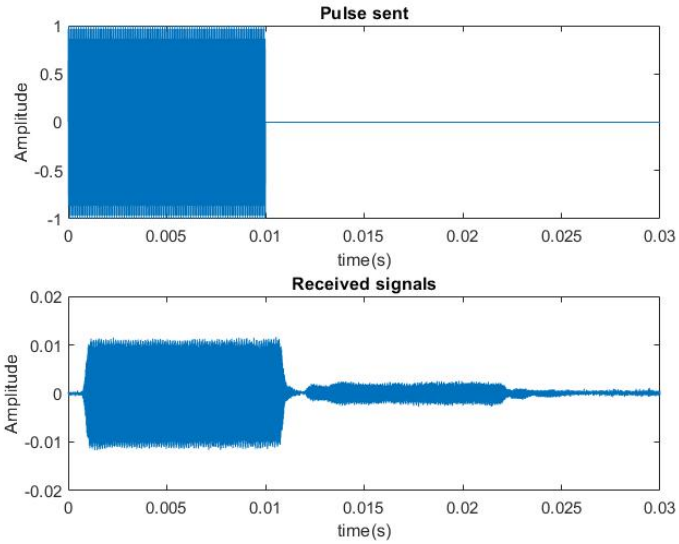

Figure 4.32: First pulse sent and received signals using the sixth version of the 3D supports.

Finally, it was performed the test in which the emitter was covered up just like it was done with the individual supports. In this case, it was verified throughout the whole test that the receiver did not detect any ultrasound. In sum, the acoustic coupling of the signal by mechanical means and by the rear of the emitter transducer were fully eliminated. In addition to this determining factor, it can also be concluded that the value of the acoustic coupling pointed out previously only has aerial origin.

Nextly, to further reduce $H_3(s)$, a upholstery sponge was glued to the main support between the emitter and the receiver as shown in figure 4.33.

Figure 4.33: 6th version with a piece of upholstery sponge between the two transducers.

The test initially performed with version 6 was repeated and the acquired values are present in

the table 4.9.Throught its analysis, it can be attested that the obtained value is inferior to the one obtained with the same version without the upholstery sponge. This result was already expected considering the results of the version 3 and version 5 where the use of sponge significantly reduced $H_3(s)$. Examining the figure 4.34 is perceptible a decrease of the amplitude of the acoustic coupling.

$\max\|RecordedSignal\|$
0.0089

Table 4.9: Maximum value in modulus of the recorded audio signal.

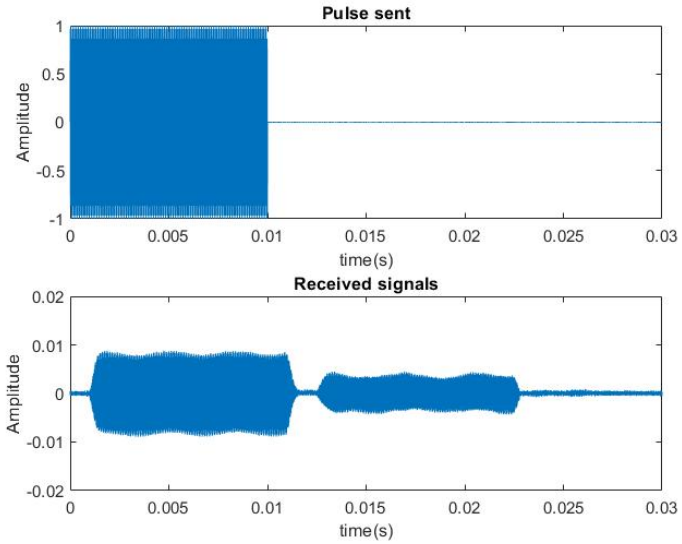

Figure 4.34: First pulse sent and received signals of the 6th version with a piece of upholstery sponge between the transducers.

4.2.7 VERSION 7

In version 6, the main support with the two individual supports along with the elastomeric foam have proven to be fundamental in reducing the acoustic coupling. For this reason, in version 7 the same idea was applied with the difference that instead of using elastomeric foam an anti-vibration pad was exploited to diminish the acoustic coupling. The anti-vibration pad is often used in industrial applications where vibration insulation is required, such as compressors, engines, and motors. This material can effectively reduce and dampen vibrations caused by machinery. That being said, this material could be a good alternative, though more expensive, to the elastomeric foam previously used.

Hence, some changes were made in the original supports from version 6 in order to accommodate the new material. To start with, the anti-vibration pad plate available had a thickness of *1 cm* and was also less dense than the elastomeric foam. Therefore, the depth of the main support was adjusted and reduced to accomodate the anti-vibration pad perfectly. Consequently, the height of the individual supports was also reduced since the previous ones were too long to be placed in the new main support (figure 4.35b). Also, taking into consideration that the anti-vibration pad was stiffer and less malleable, the flanges of the individual supports have been designed with a smaller diameter and the original notches from the main support in version 6 were removed.

Still regarding the main support (figure4.35a), the distance of *30 mm* between the center of the holes was maintained to ensure that there was sufficient material between the individual supports to attenuate $H_2(s)$.

In the following figure 4.35 it is possible to see the new designed supports with the specified changes and the respective measures.

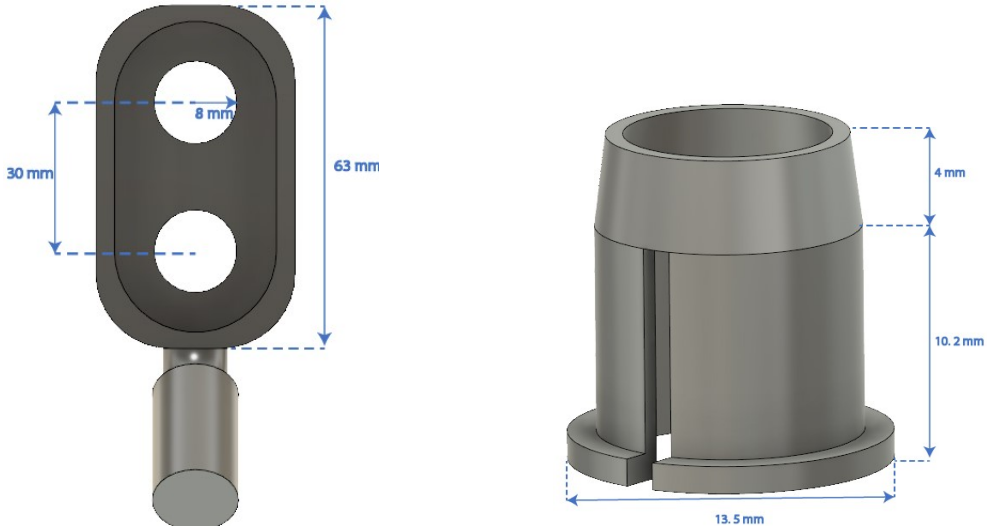

(a) Dimensions of the main support

(b) Dimensions of the individual support

Figure 4.35: 3D models of the two 3D supports from the version 7 and their dimensions.

The new printed 3D pieces are displayed in figures 4.36 and 4.37, and figure 4.38 shows the finalized version 7 with all the different components.

Figure 4.36: Main support of the version 7.

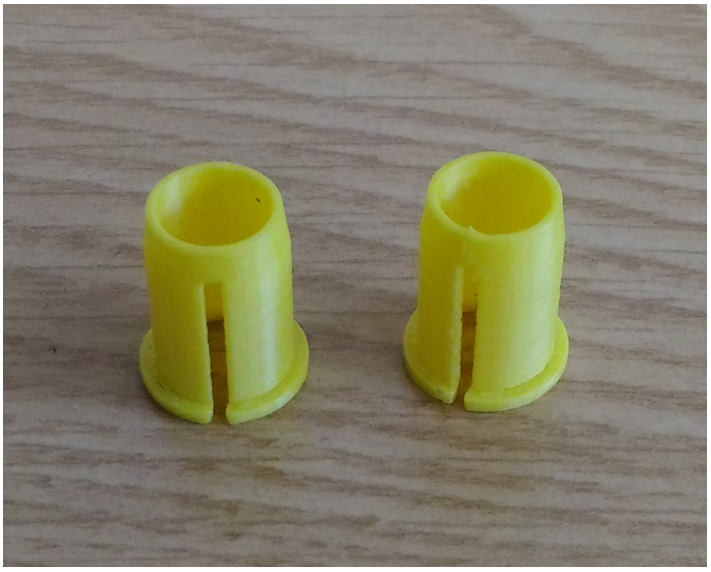

Figure 4.37: Individual transducers supports of the version 7.

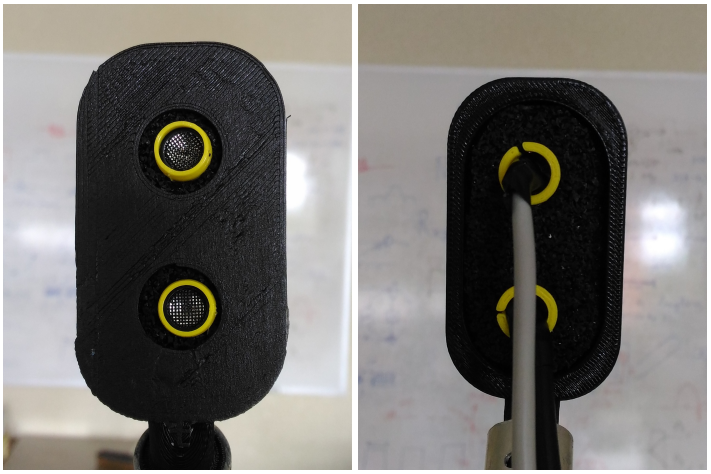

Figure 4.38: Assembly of the seventh version.

4.2.7.1 OBTAINED RESULTS

In order to test this model both tests described in section 4.1.2 were carried out. In table 4.10 are displayed the values obtained for both the variance and the maximum value in modulus of the recorded signal. Analyzing these results and comparing them with the best value obtained to date, that is, with the values obtained with version 6, these are significantly higher. In addition, by examining by figure 4.40 it is visible not only the presence of the acoustic signal coupling but also that it has a higher amplitude than the received echo. Recalling that the version 6 coupled with a piece of upholstery sponge between the two transducers the opposite effect was obtained.

$\max\lvert RecordedSignal\rvert$
0.0488

Table 4.10: Maximum value in modulus of the recorded audio signal.

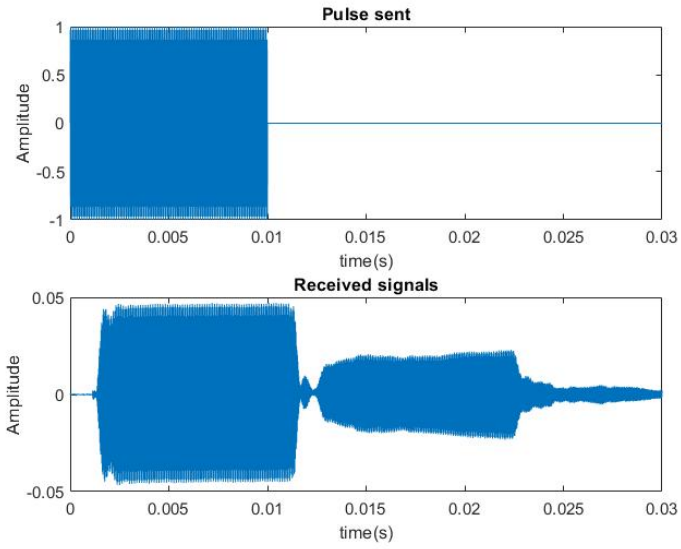

Figure 4.39: First pulse sent and received signals using the seventh version of the 3D supports.

Regarding the second test performed, it was detected during the same that contrary to what happened with the previous model, the receiver transducer was able to detect signal with a maximum value in modulus of 0.0080. Since the truncated cone of the emitter was capped the only sources of the acoustic coupling would be $H_1(s)$ or $H_2(s)$ or both.

Therefore, in order to eliminate $H_1(s)$, the same technique used during the tests of the individual supports was adopted, that is, upholster foam was placed in the rear of the transducers supports (figure 4.40). Thereafter, the second test was repeated and during this experiment the receiver transducer continued to detect signal with a maximum value in modulus of 0.0064. In this case, since both $H_1(s)$ and $H_3(s)$ were eliminated, the only possible source of acoustic coupling would be through the material ie $H_2(s)$.

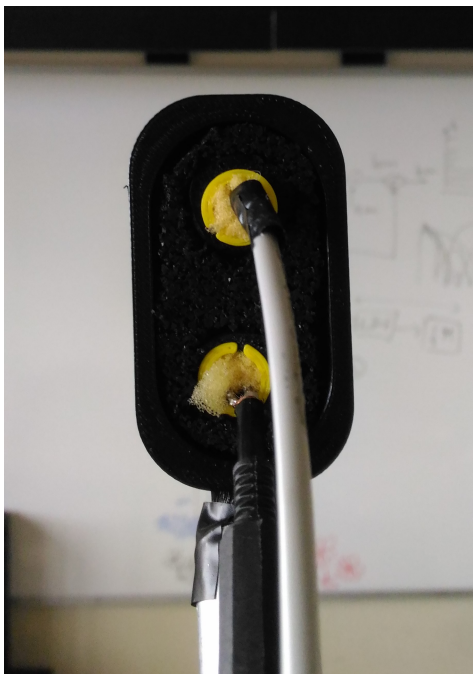

Figure 4.40: Upholstery sponge on the back of the transducers.

In general, it was concluded that although the same idea and concepts from the previous version were used to create this model, worse results were obtained. In addition, with the last test executed it was possible to conclude that part of the acoustic coupling observed was due to the material used.

Although anti-vibration pads are specially developed to attenuate and reduce the vibrations of machinery or equipment, these have proven to be ineffective at 40kHz.

4.2.8 VERSION 8

The aim beyond this version, similiarly to version 7, was to test a viable alternative to the elastomeric foam of the version 6. Hence, for the eighth version the insulation material chosen was the expansion foam due its high capacity of sound absorption. This foam is composed of polyurethane which is a material widely used in the construction field in applications such as filling of cavities, passive fire protection and thermal and acoustic insulation.

For this version, both the main and the individual supports from the version 7 were re-printed and the main support was filled with this foam. The support was left to dry overnight and since this material expandes over 30 times its original size the excess was cut off. The final result can be seen in the figure 4.41.

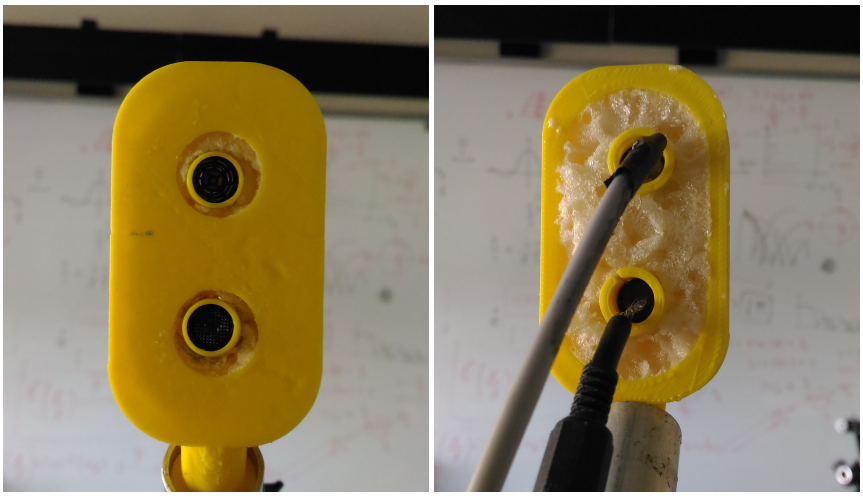

Figure 4.41: Assembly of the seventh version.

4.2.8.1 OBTAINED RESULTS

Regarding this version, the results from the first test performed are present in the following table 4.11. Among the three materials tested, using the expandable foam it was obtained the second best value regarding the maximum value in modulus which was also very close to the one obtained with the elastomeric foam of the version 6. However, when performing the second test the receiver transducer continue to detect signal with a maximum value in modulus of *0.0030*. The presence of the acoustic coupling is quite visible in the figure 4.42 where this effect has once again an amplitude higher than the echo itself.

$\max\|RecordedSignal\|$
0.0172

Table 4.11: Maximum value in modulus of the recorded audio signal.

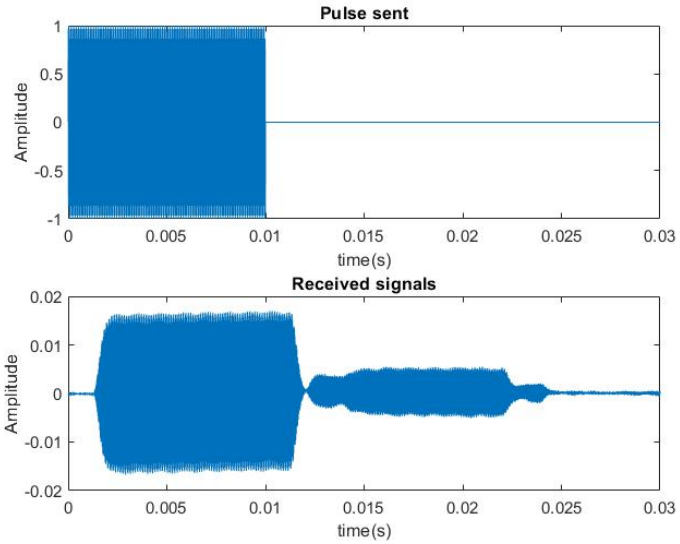

Figure 4.42: First pulse sent and received signals using the eighth version of the 3D supports.

Therefore, it was applied the same strategy which was used in the version 7, that it, to place upholster foam at the rear of the individual supports since the acoustic coupling detected could be due to $H_1(s)$ or $H_2(s)$ (figure 4.43). The second test was executed again but still the receiver transducer continued to acquire signal this time with a maximum value in modulus of *0.0016*. Since both $H_2(s)$ and $H_3(s)$ were unviable the only possible cause of the acoustic coupling would be the material used.

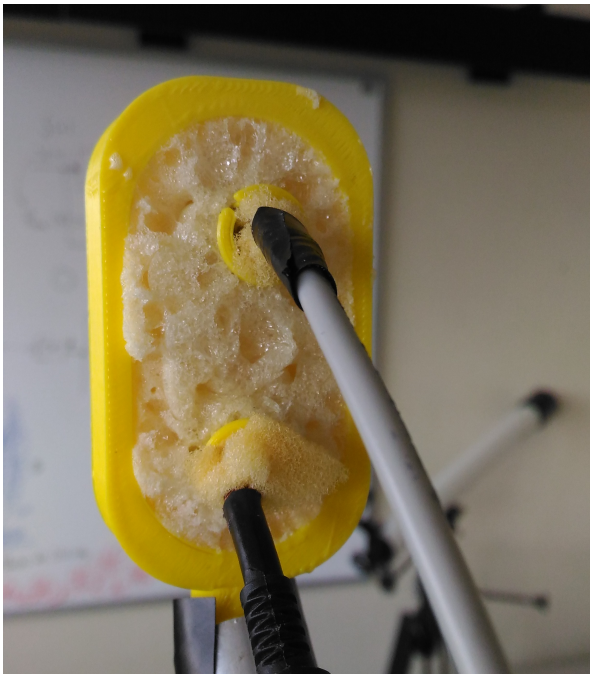

Figure 4.43: Upholstery sponge on the back of the transducers.

In this way, it is possible to affirm that even though the expansion foam did help to reduce $H_2(s)$, it was not capable of eliminating it completly like the elastomeric foam did. Therefore, it is not suitable for the context of this master thesis.

CHAPTER 5

Conclusions

In this master thesis, the aim was to minimize the acoustic coupling between the emitter and receiver transducer by designing several 3D supports for the ultrasound transducers. To begin with, it was designed a simple 3D support where it was tested the effect of the acoustic coupling at the worst-case scenario that is when both transducers were side by side without any barrier or special configuration. This first support also called as version 1 was tested and the maximum value of the recorded signal obtained was about 0.3356.

The 3D model from the first version was used to create the supports for the versions two, three and four with an increased diameter of the orifices dedicated to the transducers, so it could be possible to insert a metal tube in these in order to reduce the acoustic coupling through the air. Besides this change, in the third version several small pyramidal pieces of sponge were glued and in the fourth version in the 3D model itself, several pyramids with different weights were aleatory designed. These 3D supports were then tested for different values of *d1* and *d2* and, the best value of *0.0382* was obtained for the third version.

Since a significant part of the acoustic coupling is due to the front acoustic coupling, the focus of the fifth version was to design a new piece capable of reducing this effect even more. Therefore, in this 3D support, it was applied the Huyghens' principle and the Fourier transform to calculate the diameter of an aperture which would modify the radiation diagram of the ultrasonic transducers. If the gain at 90° is small, the effect of $H_3(s)$ is reduced. Thus, for a frequency of *40 KHz* the calculated value of the aperture was *8.575 mm* what originated two truncated cones in front of the orifices dedicated to the transducers. The new support was then designed and tested and the best obtained result of the recorded signal was *0.0512* for *d1=0.85 cm*. Even so, there were no guarantees that the acoustic coupling through the air was zero. Therefore, it was glued a piece of sponge in the middle of the support like it what was done in the second version. The tests were executed, and it was observed an overall improvement of the results over the non-sponge version. Regarding the fifth version two conclusions were taken: the aperture of *8.575 mm* reduced the acoustic coupling and that the use of an upholster sponge in the middle of the two transducers is a good solution to reduce the remaining acoustic coupling.

In the sponge and non-sponge variants from the version five, the emitter transducer was covered up to verify if the signal would still propagate by other means. In both cases, the receiver transducer continued to detect the ultrasound signal, so two individual supports based on the truncated cones

from the fifth version were created to understand it. After being tested, these allowed to conclude that a portion of the signal was propagating through the structure of the 3D piece.

All the steps and conclusions described above were essential to build the sixth version that was capable of not only eliminate the acoustic coupling through the rear of the transducers but also by mechanical means. This version consisted of a main support, two individual supports for the ultrasonic transducers and an insulation material to place inside of the main structure. Using this version, in the first test it was obtained a value in modulus of the recorded signal of *0.0120* and, when executing the second test the receiver transducer did not detect any signal. On top of that, due to the good results obtained when placing a sponge between the two transducers in versions 3 and 5, this procedure was repeated in this version. The first test was reiterated and it was obtained the best value among all the pieces drawn along this thesis which corresponds to *0.0089*.

Due to the good results obtained with the seventh version, the next step was to test the same support configuration using other insulation materials such as anti-vibration pad and expasion foam. However none of the results obtained using these materials were even close to the ones obtained with the elastomeric foam, since all of them failed in the second test.

To sum up, from all the 8 supports designed, version 6 was without a doubt the only support which solved the problem of the acoustic coupling of the signal. Thus, it is possible to conclude that the junction of a main support, the individual supports with the right apperture and the correct insulation material can indeed mitigate the negative effect of the acoustic coupling of the signal. Thanks to the significant reduction of the acoustic coupling, it is possible to measure even smaller distances using this support.

5.1 FUTURE WORK

The aim of this thesis which consisted in reducing the effect of the acoustic coupling between the ultrasonic transducers was achieved with success. Therefore, for future work, it is proposed the use of the 6th version of the transducers supports in the latest prototype of the cane and to test these two components together in real case scenarios.

References

[1] *Blindness and vision impairment*, 2018. [Online]. Available: https://www.who.int/en/news-room/fact-sheets/detail/blindness-and-visual-impairment.

[2] Y. Yi and L. Dong, "A design of blind-guide crutch based on multi-sensors", *12th International Conference on Fuzzy Systems and Knowledge Discovery (FSKD)*, 2015.

[3] R. Jafri, R. L. Campos, S. A. Ali, and H. R. Arabnia, "Visual and Infrared Sensor Data-Based Obstacle Detection for the Visually Impaired Using the Google Project Tango Tablet Development Kit and the Unity Engine", *IEEE Access*, 2017.

[4] N. Dias, *A low-cost and low-power hole-detecting cane for the visually impaired (MSc thesis)*. University of Aveiro, 2008.

[5] P. Rosa, *Bengala de apoio a cegos com detecção de buracos (MSc thesis)*. University of Aveiro, 2009.

[6] *A primeira impressora 3D portuguesa nasceu na UA e quer brilhar em Londres com a nossa ajuda*. [Online]. Available: https://uaonline.ua.pt/pub/detail.asp?c=39658.

[7] *A Dictionary of Physics*. Oxford University Press: Oxford Reference Online, 2009.

[8] H. Feng, G. Barbosa-Cánovas, and J. Weiss, Eds., *Ultrasound Technologies for Food and Bioprocessing*. Springer-Verlag New York, 2011, p. 668.

[9] D. Ensminger and L. Bond, *Ultrasonics: Fundamentals, Technologies, and Applications*, 3rd ed. CRC Press, 2011, p. 765.

[10] H. Kuttruff, *Ultrasonics : Fundamentals and Applications*, 1st ed. Springer Netherlands, 1991, p. 458.

[11] J. Bok and C. Kounelis, *Paul Langevin - From Montmartre to the Panthéon*. [Online]. Available: https://www.europhysicsnews.org/articles/epn/pdf/2007/01/epn07101.pdf (visited on 07/27/2018).

[12] *Paul Langevin*. [Online]. Available: http://www.ob-ultrasound.net/langevin.html (visited on 07/27/2018).

[13] *SONAR (Inventions)*. [Online]. Available: http://what-when-how.com/inventions/sonar-inventions/ (visited on 07/27/2018).

[14] *Weapons and Technologies - ASDIC/SONAR*, 2011. [Online]. Available: https://uboat.net/allies/technical/asdic.htm (visited on 07/27/2018).

[15] *Juno Beach Centre - Anti-Submarine Detection*. [Online]. Available: https://www.junobeach.org/canada-in-wwii/articles/anti-submarine-detection/ (visited on 07/27/2018).

[16] J. Blitz, *Ultrasonics methods and applications*. Van Nostrand Reinhold Co., 1971, p. 151.

[17] J. D. N. Cheeke, *Fundamentals and Applications of Ultrasonic Waves*, 1st ed. CRC Press, 2002, p. 480.

[18] W. Mason and R. N. Thurston, Eds., *Physical Acoustics Principles and Methods*. Academic Press, 1981.

[19] B. M. Lempriere, *Ultrasound and Elastic Waves*. Academic Press, 2002.

[20] G. Harvey, A. Gachagan, and T. Mutasa, "Review of High Power Ultrasound – Industrial Applications and Measurement Methods", *IEEE Transactions on Ultrasonics, Ferroelectrics, and Frequency Control*, vol. 61, 2014.

[21] *CC Hydrosonics - Ultrasonic Cleaning Tanks*. [Online]. Available: `http://www.cchydrosonics.com/ultrasonic-tanks.php` (visited on 10/19/2018).

[22] E. McCulloch, "Experimental and finite element modelling of ultrasonic cutting of food", PhD thesis, University of Glasgow, 2008.

[23] *Ultrasound image of a fetus at 12 weeks of pregnancy*. [Online]. Available: `https://en.wikipedia.org/wiki/Ultrasound` (visited on 10/18/2018).

[24] S. V. Ranganayakulu, N. R. Rao, and L. Gahane, "Ultrasound applications in Medical Sciences", *International Journal of Modern Trends in Engineering and Research*, vol. 3, pp. 287–293, 2016.

[25] G. T. Clement, "Perspectives in clinical uses of high-intensity focused ultrasound", *Ultrasonics*, vol. 42, pp. 1087–1093, 2004.

[26] R. Busnel, Ed., *Animal Sonar Systems*. Springer US, 1980.

[27] L. F. Mondragon, A. Vera, L. Leija, J. Gutierrez, J. E. Chong-Quero, and M. I. Gutierrez, "Transceiver system for obstacle detection based on bat echolocation with air-coupled pulse-echo ultrasound", *2017 14th International Conference on Electrical Engineering, Computing Science and Automatic Control, CCE 2017*, 2017.

[28] M. Sears, "Research Guides: Bats Echolocation", [Online]. Available: `https://guides.library.harvard.edu/bats/echolocation`.

[29] M. J. Wohlgemuth, J. Luo, and C. F. Moss, "Three-dimensional auditory localization in the echolocating bat", *Current Opinion in Neurobiology*, 2016.

[30] Asif Shaik, *SONAR or Sound Navigation and Ranging*. [Online]. Available: `http://www.physics-and-radio-electronics.com/blog/sonar-or-sound-navigation-and-ranging/` (visited on 08/23/2018).

[31] Pepperl+Fuchs, "Technology Guide Ultrasonic Sensors", Tech. Rep.

[32] M. Hersh and M. A. Johnson, Eds., *Assistive Technology for Visually Impaired and Blind People*, 1st ed. Springer-Verlag London, 2008, p. 725.

[33] J. Borenstein, I. Ulrich, and S. Shoval, "NavBelt and the Guide-Cane [obstacle-avoidance systems for the blind and visually impaired]", *IEEE Robotics & Automation Magazine*, 2003.

[34] D. Dakopoulos and N. G. Bourbakis, "Wearable obstacle avoidance electronic travel aids for blind: A survey", *IEEE Transactions on Systems, Man and Cybernetics Part C: Applications and Reviews*, vol. 40, no. 1, pp. 25–35, 2010.

[35] J. Borenstein, S. Shoval, and I. Ulrich, "Computerized Obstacle Avoidance Systems for the Blind and Visually Impaired", 2000.

[36] M. Dimitra, *Electronic Smart Canes for Visually Impaired People (BSc thesis)*, March. National and Kapodistrian University of Athens, 2018.

[37] A. R. García, R. Fonseca, and A. Durán, "Electronic long cane for locomotion improving on visual impaired people. A case study.", *Pan American Health Care Exchanges*, 2011.

[38] D. Aguerrevere, M Choudhury, and A Barreto, "Portable 3D Sound / Sonar Navigation System for Blind Individuals", 2004.

[39] J. Akita, T. Komatsu, K. Ito, T. Ono, and M. Okamoto, "CyARM: Haptic Sensing Device for Spatial Localization on Basis of Exploration by Arms", *Advances in Human-Computer Interaction*, 2009.

[40] S. Cardin, D. Thalmann, and F. Vexo, "Wearable Obstacle Detection System for visually impaired People", *VR Workshop on Haptic and Tactile Perception of Deformable Objects*, 2005.

[41] *Blavigator - Visão Sem Barreiras*. [Online]. Available: `https://sites.google.com/site/visaosembarreiras/-aplicacoes-telematicas---projectos-da-utad/blavigator`.

[42] T. Adao, L. Magalhaes, H. Fernandes, H. Paredes, and J. Barroso, "Navigation module of Blavigator prototype", *World Automation Congress (WAC)*, 2012.

[43] *UltraCane - an award winning primary mobility aid*. [Online]. Available: `https://www.ultracane.com/index.php?route=common/home`.

[44] *Miniguide Mobility Aid*. [Online]. Available: `https://www.lssproducts.com/product/Miniguide-Mobility-Aid/other-canes-and-accessories`.

[45] *'K' Sonar*. [Online]. Available: `https://abledata.acl.gov/product/k-sonar-model-1-07000-00`.

[46] R. A. Serway and J. W. Jewett, *Physics for Scientists And Engineers*, 6th ed. Thomson Brooks/Cole, 2004.

[47] T. E.o. E. Britannica, *Diffraction*. [Online]. Available: `https://www.britannica.com/science/diffraction`.

[48] R. N. Bracewell, *The Fourier Transform and Its Applications*, 3rd ed. McGraw-Hill Science/Engineering/Math, 1999.